Chapter 17

Surface Biofilm Interactions in Epizootic Shell Disease of the American Lobster (*Homarus americanus*)

Norman J. Meres

Additional information is available at the end of the chapter

http://dx.doi.org/10.5772/63498

Abstract

Epizootic shell disease (ESD) is a persistent malady that affects American lobsters (*Homarus americanus*) in the southern extent of the commercial fishery. Emerging at the turn of the 21st century, ESD presented as bacterial ulcerations on the carapace of affected lobsters. The research presented here examined the bacterial community of the lobster carapace and represented the first such attempt to characterize the lobster surface microbiome. Culture-independent techniques, such as amplicon length heterogeneity and pyrosequencing, yielded sequence data of hypervariable regions of the genes for ribosomal RNA that upon comparison revealed the likely identities of the taxa present on the lobster carapace. Although some researchers have identified a novel chitinolytic bacterium of the genus *Aquimarina* (*A. homaria*) as consistently appearing on lobsters with shell disease, this research found no evidence of a correlation of this species with the disease. Instead, analysis revealed that the genus *Aquimarina* was ubiquitous and correlated only weakly with the diseased state. The data suggest that this disease is not caused by a single pathogen but by a state of dysbiosis where normally occurring microflora emerge as potential opportunistic pathogens when there is some apparent environmental stressor that alters the interaction of the surface biofilm of the lobster.

Keywords: epizootic shell disease, lobster microbiome, next-generation sequencing, multitag pyrosequencing, amplicon length heterogeneity

1. Introduction

Since the end of the 20th century, American lobsters (*Homarus americanus*) have suffered from a host of problems that have led to morbidity and mortality. Some appear to be environmen-

tal, such as increased bottom temperatures during the summer season, and general effects of eutrophication [1]. Others are possibly the result of intoxication from anthropogenic substances [2]. Emergent pathogens, such as paramoebiasis, have significantly reduced commercially important populations in western Long Island Sound and elsewhere [1]. What makes this situation especially problematic is that the observed decline in lobster health and viability may have causes that can be linked to a convergence of environmental stressors and pathogenic microorganisms.

One such challenge to lobster health that is reducing the quality, and possibly the quantity, of commercial landings is epizootic shell disease (ESD), a condition that is manifesting itself in geographically isolated portions of the commercial lobster fishing grounds [3].

Documentation of diseases that cause lesions and ulcerations in the carapace of lobsters can be found at least as early as 1937 [4]. Initial reports of shell disease in other crustaceans are contemporary with Sindermann [5]. In many cases, the pathology appeared to be linked to degraded environments, such as the proximity to pollution sources, for example, the municipal waste dump site in an offshore canyon used by New York City where lobsters and crabs presented with shell disease [6, 7]. Another common place to find crustacean shell diseases is in commercial impoundment facilities [5]. In this situation, chitinolytic bacteria appeared to be eroding the carapace faster than it could be replaced by molting, leading to a pitting of the cuticle. However, there has only been one report of an infectious process after the lobster's carapace was abraded and swabbed with *Vibrio* sp. [8]. Waddy et al. described the integument during the intermolt phase as consisting of four layers, beginning externally: the epicuticle, the exocuticle, the endocuticle, and the membranous layer [9]. Beneath these four layers are the epidermis, the basement membrane, and the connective tissue. The transport to the epicuticle of extracellular substances, presumably with protective properties, from the epidermis occurs through pore canals that transverse the exoskeleton. All but the membranous layer is calcified either with regularly organized calcite crystals or with amorphous calcium carbonate and all but the epicuticle contains the acetyl-aminated polysaccharide, chitin.

In the epicuticle, calcification consists of spherulitic calcite surrounded by a lipid-protein matrix; in the exocuticle and endocuticle, calcite crystals are dispersed throughout chitin-protein fibers that are referred to as lamellae. In addition, the exocuticle contains trabeculae that are composed of apatite (calcium phosphate) that resembles spongy bone tissue in vertebrates [10]. The endocuticle is the most calcified layer of the exoskeleton [11].

According to Smolowitz et al. [3], ESD is identifiable by erosions of the carapace that have a unique histology. The presence of lesions on the carapace of an infected lobster is the most visible sign of the disease. Histological examination revealed bacteria as the most common organisms in the lesions, whereas some protist constituents were found in more advanced cases. The lesions were grouped into three categories based on the depth of the bacterial incursion, presuming that depth reflects a progressive erosion of the cuticle.

Category 1 is the least severe erosion, with shallow lesions extending into the epicuticle and exocuticle. The margins of the lesions often exhibited evidence of melanization, but inflam-

http://dx.doi.org/10.5772/63498

mation in the underlying connective tissue or other evidence of an immune response is rarely observed at this stage. Bacteria are found in the leading edges of the lesion and in the crystalline chitin lattice.

Category 2 lesions are moderately deep, penetrating the calcified endocuticle. The crystalline lattice structure of the chitin takes on a "pillar-like" appearance as the bacteria degrade the protein structure between the lattice crystals. The endocuticle exhibits melanization, especially in the vertical areas of bacterial incursion. Evidence of immune response to the infection includes inflammation of the underlying cuticular epithelium and "moderate numbers" of hemocytes in the tissues. Secondary invasion by small protists occurs during this stage. These organisms are apparently responsible for the degradation of the crystal lattice structure of the chitin. In some category 2 lesions, an "inflammatory cuticle" forms between the uncalcified endocuticle and the cuticular epithelium. The latter has some areas of hyperplasia and hypertrophy.

Deeper erosions into the uncalcified endocuticle are characterized as category 3 lesions. At this stage, the overlying structures of the carapace are absent, and the exposed areas are melanized. The cuticular epithelium is hyperplastic and hypertrophic and exhibits an intense inflammatory response accompanied by greater hemocyte infiltration. The underlying connective tissue also exhibited signs of inflammation and immune response. The most extreme types of category 3 lesions had no more tissue than the inflammatory cuticle overlying the cuticular epithelium. In some cases, the lesions progressed to ulcerations, which were characterized by a complete absence of cuticular tissue and cuticular epithelium. Degranulated hemocytes developed a multilayered pseudomembrane to cover the connective tissue. The outer layer of the pseudomembrane was necrotic and melanized.

Certain groups of bacteria have been found as common constituents on the carapaces of moribund lobsters, and overall populations of bacteria are higher than on the carapaces of healthy lobsters [11]. Using a combination of culture-dependent techniques, polymerase chain reaction (PCR), and denaturing gradient gel electrophoresis, the group of Chisosterdov isolated three novel bacteria that were ubiquitous in ESD lesions: *Aquimarina homaria* I32.4, *Thalassobius* sp. 131.1, and *Pseudoalteromonas gracilis* ISA7.3 [11]. Quinn et al. [12] were successful at initiating lesions that are histologically similar to ESD in captive lobsters using these three bacteria. The abrasion of the carapace was necessary for lesions to form. Researchers were also able to isolate *A. homaria* from lesions in "diet-induced" shell disease. These lobsters were fed strictly herring and were deprived of sources of astaxanthan, rendering them nearly colorless [13].

The characterization of microbial communities using terminal restriction fragment length polymorphism revealed that, although no grossly significant difference in communities on healthy lobsters was present compared to diseased lobsters, there were some minor differences [14]. More anaerobic bacteria and greater numbers of α- and β-proteobacteria were found in the lesions. Bell et al. used lobsters from eastern and western Long Island Sound. Lobsters from a coastal Maine site were used as reference specimens. This study also elucidated the activities of four bacterial ectohydrolases on shell samples from healthy and diseased specimens and found that, whereas chitinase activity was high in all samples, cellulase and

proteinase activities were significantly higher in diseased specimens. Lipase activity was higher in Long Island Sound lobsters compared to those from Maine but was apparently similar between healthy and diseased lobsters. They concluded that chitin degradation was not as important to the progression of the disease as the degradation of lipids and protein in the carapace. Bell et al. [14] interpreted the spatial difference in lipase activity in bacteria to indicate that the degradation of the lipid moieties in the epicuticle may be an important initial step in disease progression and hypothesized that it should correlate positively with geographic areas of ESD prevalence.

The works of Smolowitz et al. [3] and Bell et al. [14] make clear that ESD differs from earlier types of shell disease. ESD is ostensibly bacterial in origin, but other research indicates that the bacterial infection may only be a proximate cause.

Shields et al. [15] found that some idiopathic conditions were more prevalent in lobsters from Rhode Island compared to lobsters from Maine. Rhode Island lobsters presented with vibriosis, hepatopancreatitis, and eye lesions at a significantly higher rate than did Maine lobsters. When Rhode Island lobsters with and without ESD were compared, these and other idiopathic conditions were present but did not occur more frequently in lobsters with the disease.

Laufer et al. [16] found that ESD lobsters had higher levels of alkylphenols than did unaffected lobsters and that bottom sediments had higher than normal levels of these compounds in areas where diseased lobsters resided. Using gas chromatography-mass spectrometry, Laufer et al. identified four alkylphenol species: 2-*t*-butyl-4-(dimethylbenzyl) phenol, 2,6-bis-(*t*-butyl)-4-(dimethylbenzyl) phenol, 2,4-bis-(dimethylbenzyl) phenol, and 2,4-bis-(dimethylbenzyl)-6-*t*-butyl phenol. The second compound, 2,6-bis-(*t*-butyl)-4-(dimethylbenzyl) phenol, was developed but never used by Monsanto Corporation as a mosquito larvicide. Biggers and Laufer [17] have identified alkylphenols as endocrine disrupters having juvenile hormone activity. This hormone, also referred to as methyl farnesoate in crustaceans, is important to the metamorphosis of larvae [18]. Laufer et al. [19] confirmed that alkylphenols do inhibit larval development in lobsters. In adult lobsters, however, these compounds displace tyrosine molecules and delay the hardening of the shell by preventing the tyrosine cross-linking of proteins and chitin [19]. Kunkel et al. [10] found that, in lobsters with ESD, the exocuticular apatite layer was greatly reduced or absent. Another group of researchers found that several measurements of immune response in lobsters, including phenoloxidase activity and antimicrobial activity of the hemolymph, phagocytic activity, and reactive oxygen species production, was depressed in lobsters from eastern Long Island Sound (one of the prime ESD areas) compared to lobsters from western Long Island Sound and Maine [20].

Tarrant et al. found that lobsters with ESD had gene expression patterns that were consistent with exposure to xenobiotics. Specifically, they found an elevated expression of ecdysteroid receptors and elevated expression of CYP450 (a cytochrome *P*450 moiety that is positively correlated with increased ecdysteroid levels). In addition, decreased arginine kinase expression in thoracic muscles was observed in lobsters presenting with ESD. Arginine kinase is analogous to creatine kinase in vertebrates [21]. These findings suggest that lobsters from Rhode Island waters that were sampled for these studies were subjected to atypical environmental stress factors.

http://dx.doi.org/10.5772/63498

In response to the ESD crisis, a group of scientists, fisheries managers, and lobstermen formed the New England Lobster Health Initiative. It was this ad hoc committee that ultimately received funding that was awarded to several university and institutional researchers, including the award that funded the study reported here. The findings of each group were published as a special edition of the *Journal of Shellfish Research* [22]. Included in that edition was an article that summarizes some of what is contained herein [23].

A systems approach to ESD was employed in this study to elucidate the surface biofilms of lobsters in three states of health: Healthy, Diseased, and Healthy-on-Diseased (areas of the carapace on a lobster presenting with ESD that do not yet have the characteristic lesions). Using culture-independent molecular techniques coupled with multivariate statistical and network analysis models, this study surveyed the biofilms of the carapaces of lobsters from the geographic area that is most affected by ESD.

This study represents the first survey of the surface microbiome of the American lobster. Although the sequencing techniques can provide a comprehensive overview of bacteria in a sample, this study cannot be regarded as a global assessment of the lobster microbiome. The lobsters surveyed here are from a one geographic location and represent a statistically small sample of lobsters. Elucidating the complete lobster microbiome should make use of lobsters from as much of the natural range as possible and should include a statistically large sample of specimens. Bell et al. [14], for example, have demonstrated that there is a biochemical activity in the lobster surface microbiome that varies geographically.

This survey does, however, offer a glimpse into the subtle microbiome differences between lobsters that present with ESD ("Diseased") and those that do not ("Healthy"). In addition, a third class, "Healthy-on-Diseased," has been defined as a region of the shell of a lobster with ESD that does not present with lesions. This third class may provide some insight into the disease progression.

As described previously, Quinn et al. [12] were successful in initiating lesions similar to ESD with three bacteria that were isolated from ESD lesions. Some of the infections were initiated with only one bacterium (*A. homaria*), whereas other lesions were initiated as "coinfections" with *Thalassobius* sp. and *P. gracilis*. The removal of the epicuticle by abrasion was necessary to initiate the infection. These authors acknowledge that ESD lesions present with many more bacteria and that ESD appears to be a polymicrobial disease.

The polymicrobial nature of ESD, and the desire to illuminate something of its etiology, is the focus of this research. To that end, culture-independent techniques were employed to elucidate the bacterial community, and multivariate statistics were used to interpret the results. Specifically, length heterogeneity-PCR (LH-PCR) was used to survey a typical lobster. This provided an overview of the distribution of bacteria on different regions of the lobster carapace. LH-PCR data do not provide sequence information but identify PCR amplicons by size (basepair length) that indicate different taxa. The number of representative fragments found in the cephalothorax region of the carapace, combined with the knowledge that this region had the highest incidence of ESD lesions, led to the decision to focus the next phase of molecular interrogation on the cephalothorax. This phase used multitag pyrosequencing (MTPS) to

generate raw sequence data of each PCR amplicon, which could be identified by comparing these sequences to known sequences in a standard database.

Discriminant analysis (DA) was chosen as a means of determining if there is a statistically significant difference between the bacterial communities found on the three classes of data (Healthy, Diseased, and Healthy-on-Diseased). In addition, DA assigns each variable (bacterial taxon) with coefficients that indicate its contribution to the discriminant function. Correlational network analysis, which uses techniques similar to social network analysis to create a visual image of correlations between the bacterial taxa, was employed to identify which taxa are positively and negatively correlated in each of the three states examined. Using correlational difference analysis to compare the states, it may be possible to more clearly identify the changes in bacterial population on the lobster carapace that are correlated with a decline in health.

We approached the problem using the following hypothesis:

H: The bacterial communities on lobsters with ESD are significantly different in quality and quantity than unaffected lobsters.

HA: The bacterial communities on the carapaces of healthy and shell-diseased lobsters are similar.

2. Materials and methods

2.1. LH-PCR

We initially performed a survey of the microbiome on normal lobsters using a culture-independent method to characterize the taxa composition of the biofilm on various locations of the lobster shell. Characterizing a microbial population using molecular techniques is advantageous over culture-dependent techniques in that the latter relies on the growth of bacteria on artificial media usually at a controlled temperature. Many bacteria have particular nutritional and environmental conditions that render them difficult to grow in laboratory cultures and would not be present in cultures taken from the environment. Existence in culture medium, as discussed in the previous chapter, requires that the bacteria assume a planktonic phase rather than embedding in a biofilm, which may be an abnormal state for most species [24]. These molecular techniques are sometimes referred to as "culture independent" in that they identify bacteria from a sample without first attempting to grow them under artificial conditions. Identifying bacteria by amplifying and sequencing the entire genome of each individual would be impractical and inordinately time-consuming. Several techniques exist that enable the identification of bacteria by taking advantage of variable regions within genes that are ubiquitous in all prokaryotes. This research used the first two variable regions of the genes encoding for the small (16S) subunit of ribosomal RNA (rRNA) to discriminate between different operational taxonomic units (OTUs) that are surrogates for taxa identification. There are nine such variable regions within this gene.

The technique employed in this research is called LH-PCR [25]. The variability, or heterogeneity, of the basepair lengths of the variable regions can be used to define the OTUs that represent individual taxa, but the technique does not assign a taxon name to them.

An LH-PCR survey of the diversity of the bacteria in the shell microbiome of a store-bought lobster was initially performed to determine the compositional patterns throughout the surface of the lobster. In this procedure, bacterial DNA was extracted from various regions of the lobster carapace (claw, abdomen, cephalothorax, and telson). The carapace samples were dissolved in EDTA and proteinase K to recover all microorganisms from the surface and subsurface, and DNA was extracted using the FastDNA Spin Kit (MP Biomedicals, Solon, OH). PCR was employed to amplify the bacterial genes for the first two hypervariable regions (V1 and V2) of the 16S rRNA subunit using universal primers 27F (5'-AGA GTT TGA TCM TGG CTC AG-3') and 355R (5'-GCT GCC TCC CGT AGG AGT-3'; Invitrogen Corporation, Carlsbad, CA) [26].

The LH-PCR products were diluted according to their intensity on agarose gel electrophoresis and mixed with ILS-600 size standards (Promega, Madison, WI) and HiDi Formamide (Applied Biosystems, Foster City, CA). The diluted samples were then separated on an ABI 3130xl fluorescent capillary sequencer (Applied Biosystems) and processed using the Genemapper™ software package (Applied Biosystems). Normalized peak areas were calculated using a custom PERL script, and OTUs constituting less than 1% of the total community from each sample were eliminated from the analysis to remove the variable low abundance components within the communities.

2.2. MTPS

The technique described above employed a culture-independent technique that is capable of resolving amplified fragments of DNA by size (OTUs). This can be useful in making observations on gross changes of microbial communities over time, such as in a site that is contaminated by petroleum or some other organic material. In this case, LH-PCR was used to demonstrate that the biofilm on the cephalothorax was the best representative sample of the shell microbiome. The next phase of interrogation employed MTPS [27] to further elucidate the nature of the microbial community. The OTUs from the lobster samples were sequenced using next-generation sequencing technology, and the sequence reads were matched as closely as possible to known bacterial taxa. This provided us with data that could be used in a variety of ways to demonstrate the correlation between bacterial taxa and various states of health in the lobster.

Cuticle samples (0.5 cm^2) were harvested as part of the "100 Lobsters" Project [28] and in a manner described therein. The lobsters were collected from within Narragansett Bay, Rhode Island. A total of 55 lobsters had ESD, whereas 47 were categorized as apparently healthy (i.e., the lobsters did not have visible ESD lesions). The samples were shipped in plastic vials on dry ice and stored at -80°C until processed. Three types of carapace samples were taken: those from lesions of diseased lobsters (Diseased), those from lesion-free areas of diseased lobsters (Healthy-on-Diseased), and those from apparently healthy lobsters (Healthy). The carapace samples were dissolved in EDTA and proteinase K to recover all microorganisms from the

surface and subsurface, and DNA was extracted using the FastDNA Spin Kit (MP Biomedicals).

PCR was employed to amplify the bacterial genes for two hypervariable regions of the rRNA subunit using modified primers 27F (5'-AGA GTT TGA TCM TGG CTC AG-3') and 355R (5'-GCT GCC TCC CGT AGG AGT-3'; Invitrogen Corporation). The forward primer listed above was modified with a "barcode" sequence that was unique to each DNA sample extracted from individual lobsters, allowing us to track the various bacterial sequence reads to their specific sample origin (i.e., the lobster and carapace region from which the bacteria were sampled). MTPS was employed to characterize the microbiome from a subset of the carapace samples that were used in the LH-PCR analysis. We generated a set of 96 fusion primers that contained the emulsion PCR linkers (454 Life Sciences) on the 27F and 355R universal 16S rRNA primers along with different eight-base "barcodes" on the 27F primer. Each lobster DNA sample was then amplified with a unique set of tagged 16S rRNA primers, pooled, subjected to emulsion PCR, and pyrosequenced using a GS-FLX pyrosequencer as per manufacturer's instructions (Roche, Branchburg, NJ). Data from the pooled sample were "deconvoluted" by sorting the sequences into sample bins based on the barcodes using custom PERL scripts. This technique allows the rapid sequencing of multiple samples at one time, yielding thousands of sequence reads per sample. The sequence reads were identified using the Bayesian analysis from the Ribosomal Database Project [29]. We used a custom PERL script to normalize the abundances of the taxa in a sample based on the total reads in that sample.

The sequences were aligned that were identified as *Aquimarina* spp. using the RDP 10 analysis [29] with reference sequences available in GenBank and constructed a neighbor joining tree for the genus. The clades in the tree were labeled by the major species present therein. Dr. Andrei Chisosterdov, a colleague from Louisiana State University and a participant in the New England Lobster Health Initiative, supplied an rRNA sequence for *A. homaria*. None of the bacteria from our samples that were identified as members of the genus *Aquimarina* were greater than 95% similar to Dr. Chisosterdov's reference sequence, indicating that we identified similar examples of the same genus.

The software program Quantitative Insights into Microbial Ecology (QIIME) [30] was used to compare the microbial communities on the three types of carapace samples and to construct a UniFrac neighbor joining tree that graphically displays the similarities in microbiome structure between each lobster sample in the study. The technique was validated using jackknifing to estimate the dispersion of the data [31]. According to Lozupone and Knight [32], the UniFrac metric "measures the phylogenetic distance between sets of taxa in a phylogenetic tree as a fraction of the branch length that leads to descendents from either one environment or the other, but not both." In the process, UniFrac was able to depict the evolutionary differences between environments. In this application, UniFrac was used to compare phylogenetic differences between bacterial communities and provide a graphic representation of the differences. Each terminal node, therefore, represents a unique phylogenetic tree of that sample. The distance between the nodes is the distance between these trees.

http://dx.doi.org/10.5772/63498

2.3. DA

DA, sometimes referred to as discriminant function analysis, is a multivariate statistical method that identifies variables of different cases that are useful in the discrimination of those cases into different classes. The analysis of the data results in the construction of a linear equation in which the variables are factors of both unstandardized and standardized coefficients. The products of these variable coefficient pairs are summed to produce a score for each case, and that score determines the membership of that case in a specific class [33]. The summation of the unstandardized coefficients includes a constant. Standardizing the coefficients eliminates the constant. These coefficients are partial coefficients that compare the relative importance of the independent variables [34]. We define the cases as individual lobsters in the study and the variables as the bacterial taxa that were identified by MTPS.

In addition to producing unstandardized and standardized linear coefficients that can be used to discriminate classes, DA produces full coefficients that are referred to as structure coefficients. These are measurements of the importance of the independent variables and the discriminant function itself [34, 35]. Structure coefficients are a more definitive coefficient for determining relative importance of the variables [35]. In this research, the structure coefficients are useful in providing us with a ranking of the variables, which reflects their relative importance to ESD.

The abundance data for the 170 variables (taxa) from the 102 lobster samples were analyzed by DA with PASW version 18 (IBM, Chicago, IL). In the first analysis, we compared the taxa on the cuticle from Diseased versus Healthy animals, the second analysis compared the taxa on the cuticle from Diseased animals versus Healthy-on-Diseased animals, and the third analysis compared the taxa on the cuticle from Healthy animals versus Healthy-on-Diseased animals.

2.4. Correlational network analysis

The computations described above are useful in identifying variables (bacterial taxa) that are likely candidates for determining the class of each sample, in this case, the state of health of the lobster being sampled. DA, however, does not account for the effects of one variable upon another. The members of a microbial community interact not only with their host or source of food but also with each other [36].

Network analysis is a statistical-graphical technique that has wide applications in fields as diverse as the social sciences and epidemiology and has gained some popularity among people working in "homeland security." Arguably the most common of these types of applications is social network analysis, which can be defined as a "study of human relationships by means of graph theory" [37].

Microbes occupying a biofilm are exposed to the biochemical output of their neighboring microorganisms. Some of these molecules are metabolic wastes of one microbe but serve as nutritive material for another, which can be viewed as metabolic cooperativity [36]. Members of a community also secrete antimicrobial agents in an effort to reduce competition, and still

other bacteria engage in quorum sensing, the detection of chemical signals as a means of monitoring population density [36]. It would be incorrect to equate human interactions with those of microorganisms, but it is arguably valid to recognize that biofilms exhibit a social structure that is mediated via biochemical signaling. Therefore, network analysis has the potential to elucidate microbial interactions within a biofilm. Within this study, the chemical interaction between various members of the biofilm was not directly investigated. Instead, we calculated the statistical correlations between bacterial taxa as a means of inferring their interactions and relationships.

The pyrosequencing abundance data were analyzed using Spearman rank correlation using a custom R module [38]. Spearman rank correlation is a nonparametric statistical function that allows the comparison of nonlinear data [36]. All possible correlation coefficients between variables are calculated, and correlations between variables are ranked in an output table. The parameters for the ranking were set as follows: $p \leq 0.01$, four minimum pairs per variable (taxa) and five minimum nonzero pairs.

The correlation tables were generated by the R module into the networking software Cytoscape [39] version 2.8.2 to construct correlational network diagrams of the three states of health of the lobster microbiome: Diseased, Healthy, and Healthy-on-Diseased. In addition, the data were used to construct correlation difference networks that plot edges between features whose correlations have significantly changed between the two states being compared. One can interpret these correlation difference networks as a depiction of what correlations were altered between the two states. The author constructed two such maps: Healthy versus Diseased and Healthy-on-Diseased versus Diseased.

3. Results

3.1. LH-PCR

Initially, the lobster carapace was surveyed to determine the bacterial community distribution on various regions of the carapace. **Figure 1** is a histogram of the normalized abundance of OTUs that were present on the various regions of the carapace (pink and red: cephalothorax, yellow: claws, green: abdomen, and tail: blue). The LH-PCR profiles revealed that, with a few exceptions, the OTUs present on the cephalothorax are representative of the microbiome present on other regions, such as the claw and the abdomen. Of the 29 OTUs identified, 22 are present on the cephalothorax, 17 are present on the claws, 17 are present on the tail (telson), and 13 are present on the abdomen. Using the Shannon index of diversity [40], the cephalothorax region had a index of 2.81 and an eveness score of 0.85. The claw region had an index value of 2.80 and a eveness score of 0.833. The tail had an index value of 2.37 and an eveness score of 0.75. The abdomen had an index value of 1.95 and a eveness score of 0.61.

The peaks in the fingerprints are described as OTUs, because this method alone does not identify the bacteria. In fact, a peak may contain more than one species, and strains of the same species may show up in different peaks. The normalized OTU abundance for each sample was

http://dx.doi.org/10.5772/63498

plotted as a stacked histogram to demonstrate the distribution of the microbiome on the lobster carapace.

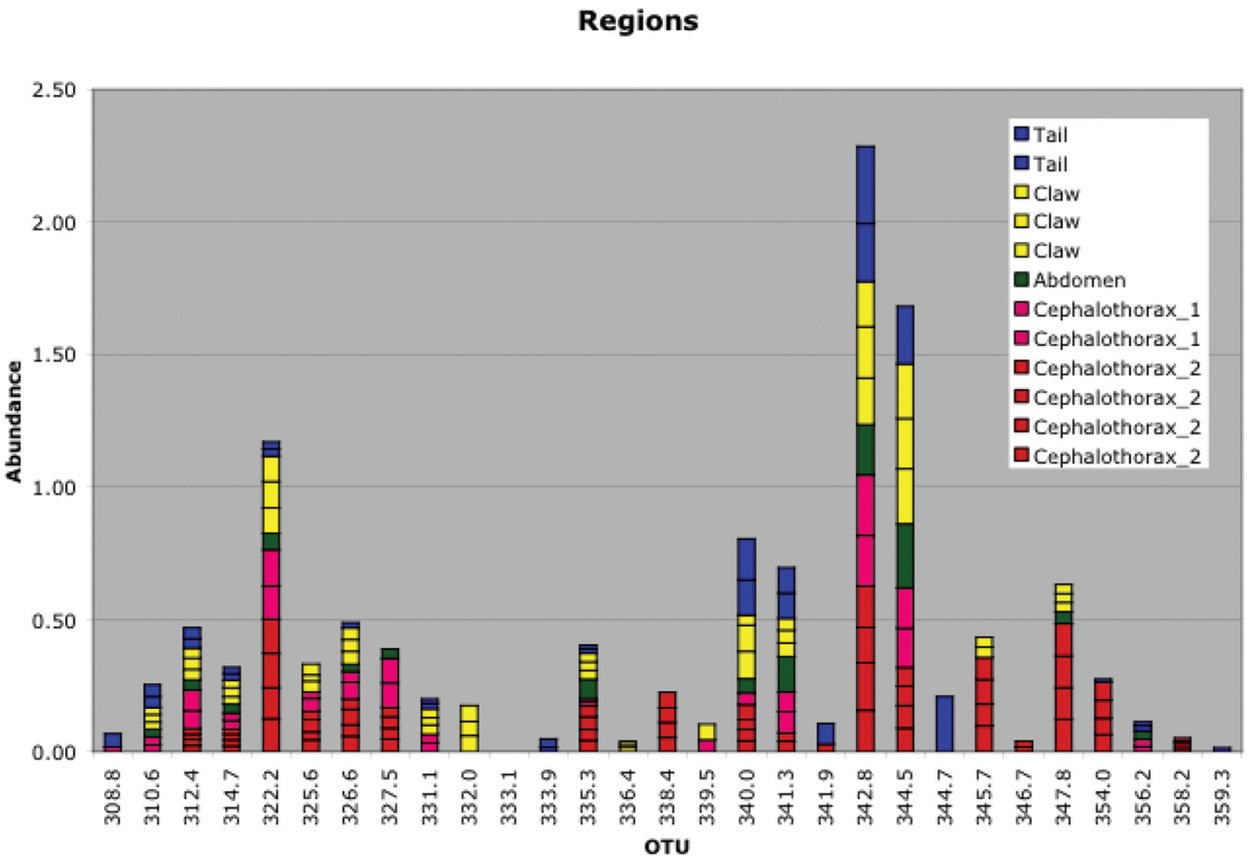

Figure 1. Replicate LH-PCR fingerprint analysis of various regions of the carapace. The normalized OTU abundance for each sample was plotted as a stacked histogram to demonstrate the distribution of the microbiome on the lobster carapace. Multiple bars of the same color represent OTU abundances from several samples of the same region of the shell. Therefore, OTU abundances from multiple samples may add up to greater than 100%.

3.2. MTPS

MTPS was performed on 102 lobster samples and the resulting sequence reads were sorted based on their tags or barcodes. The analysis yielded 212,019 reads with an average of 1594 reads per sample. We identified 170 bacteria present on the cuticle of lobsters from Narragansett Bay, Rhode Island, having culled taxa that were less than 1% of the total community under the *a priori* assumption that rare taxa will not contribute to the disease process. Of these 170 bacteria, 167 were identified to the level of genus, 1 was identified to the level of family, and 2 were identified as OTUs whose complete identities are unknown.

Figure 2 is a histogram of the average abundance of the taxa found in each sample class (i.e., Diseased, Healthy-on-Diseased, and Healthy) rank ordered by the average abundance of the Disease class (red bars). The entire histogram for all 170 taxa is depicted in the insert. The most abundant taxa found in the carapace microbiome include the genera *Jannaschia*, *Aquimarina*,

Cardiobacterium, *Thalassobius*, and *Loktanella* and the suborder *Micrococcineae*. However, essentially all genera are found in all disease classes (i.e., Healthy, Healthy-on-Diseased, and Diseased).

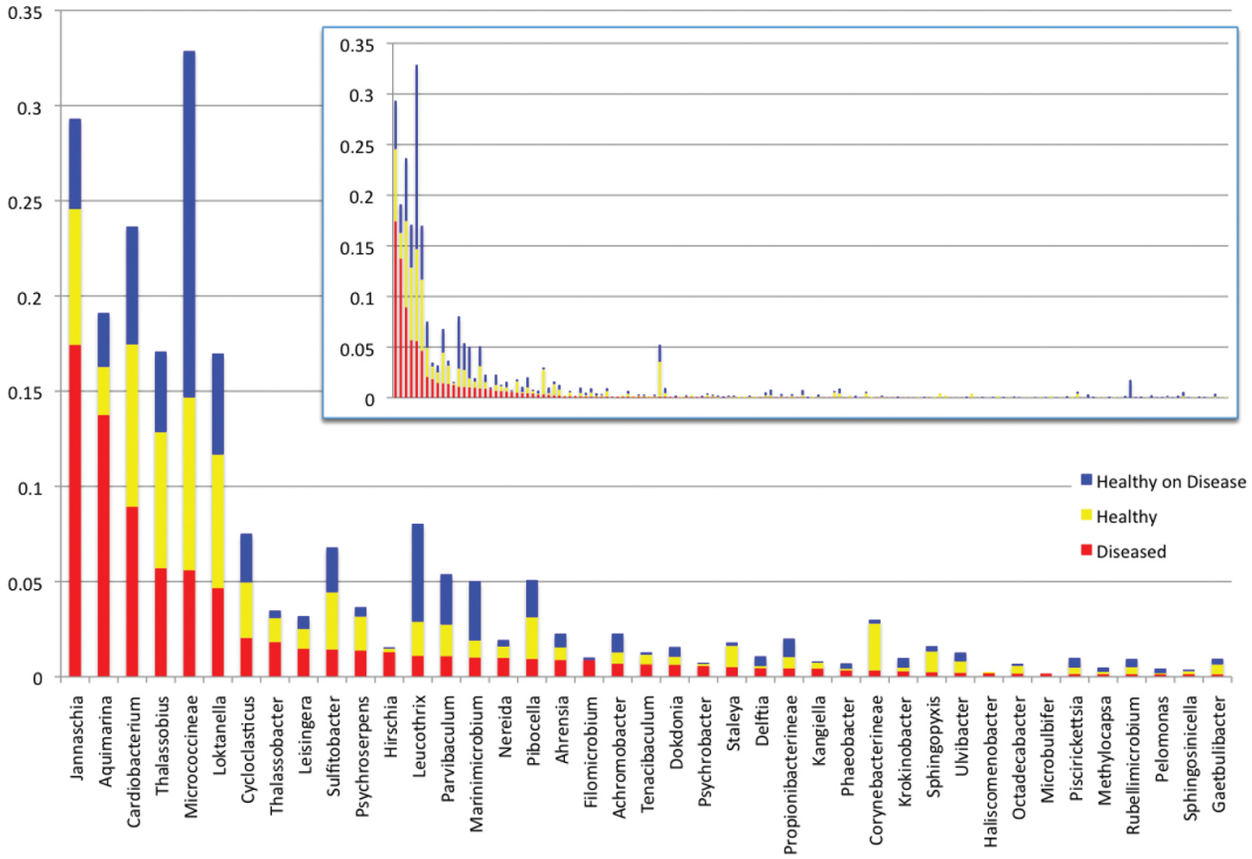

Figure 2. MTPS analysis of the cephalothorax microbiome. The normalized abundances of the most prominent taxa found on the cephalothorax of 102 lobsters is plotted as a histogram, rank ordered by those taxa in the disease state. The histogram of all 170 taxa is plotted in the insert.

Figure 3 is a neighbor joining tree that displays all of the members of the genus *Aquimarina* that were found in GenBank along with all the *Aquimarina* sequences found in these lobster samples. They are labeled according to their sample origin, and clades were labeled by the most abundant identified species in that clade. This tree is included here to illustrate the diversity of the genus and to demonstrate its ubiquity in samples of all three sampling classes of this study. There are three clades in that represent known *Aquimarina* species: *A. intermedia*, *A. mulleri*, and *A. laterculi*. We see an additional two clades that represent previously identified *Aquimarina* species. In addition, we can see that there are at least three clades of previously unidentified *Aquimarina* species (unlabeled clades). There are representatives of Healthy, Healthy-on-Diseased, and Diseased samples in all clades.

http://dx.doi.org/10.5772/63498

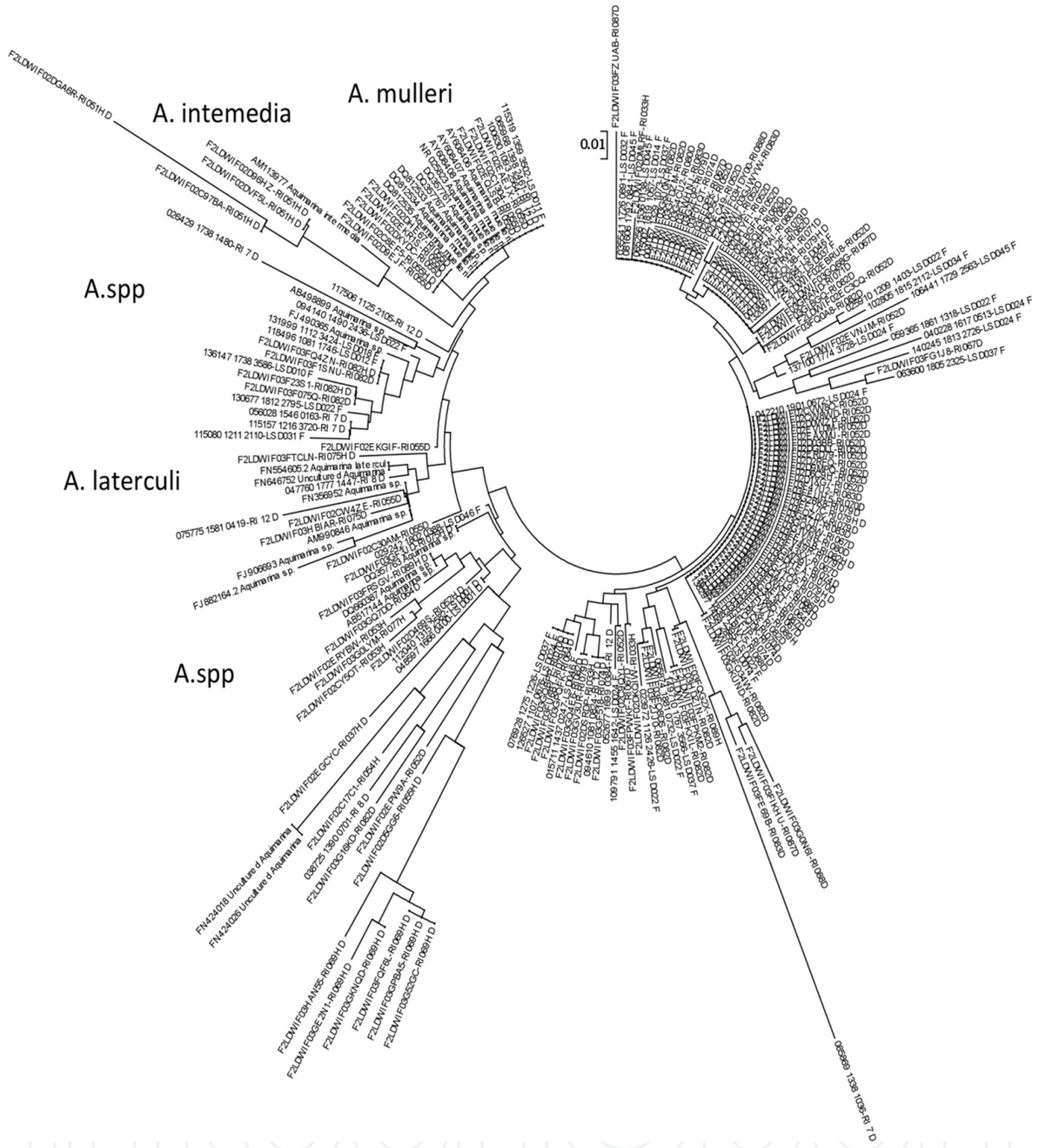

Figure 3. Neighbor joining tree of *Aquimarina* spp. identified in the lobster microbiome.

The weighted UniFrac tree is displayed in **Figure 4**. Although a cursory inspection of the figure may lead one to conclude that there is indeed a clustering of the three disease classes (Diseased, Healthy, and Healthy-on-Diseased), significance tests reveal that the differences between the three classes are not significant (Diseased vs. Healthy-on-Diseased: p=0.45, Diseased vs. Healthy: p=1.0, and Healthy-on-Diseased vs. Healthy: p=0.85). This demonstrates that, although there is some clustering, there is no clear separation between the three disease classes (Diseased, Healthy, and Healthy-on-Diseased), that is, they are more or less equally distributed throughout the neighbor joining tree.

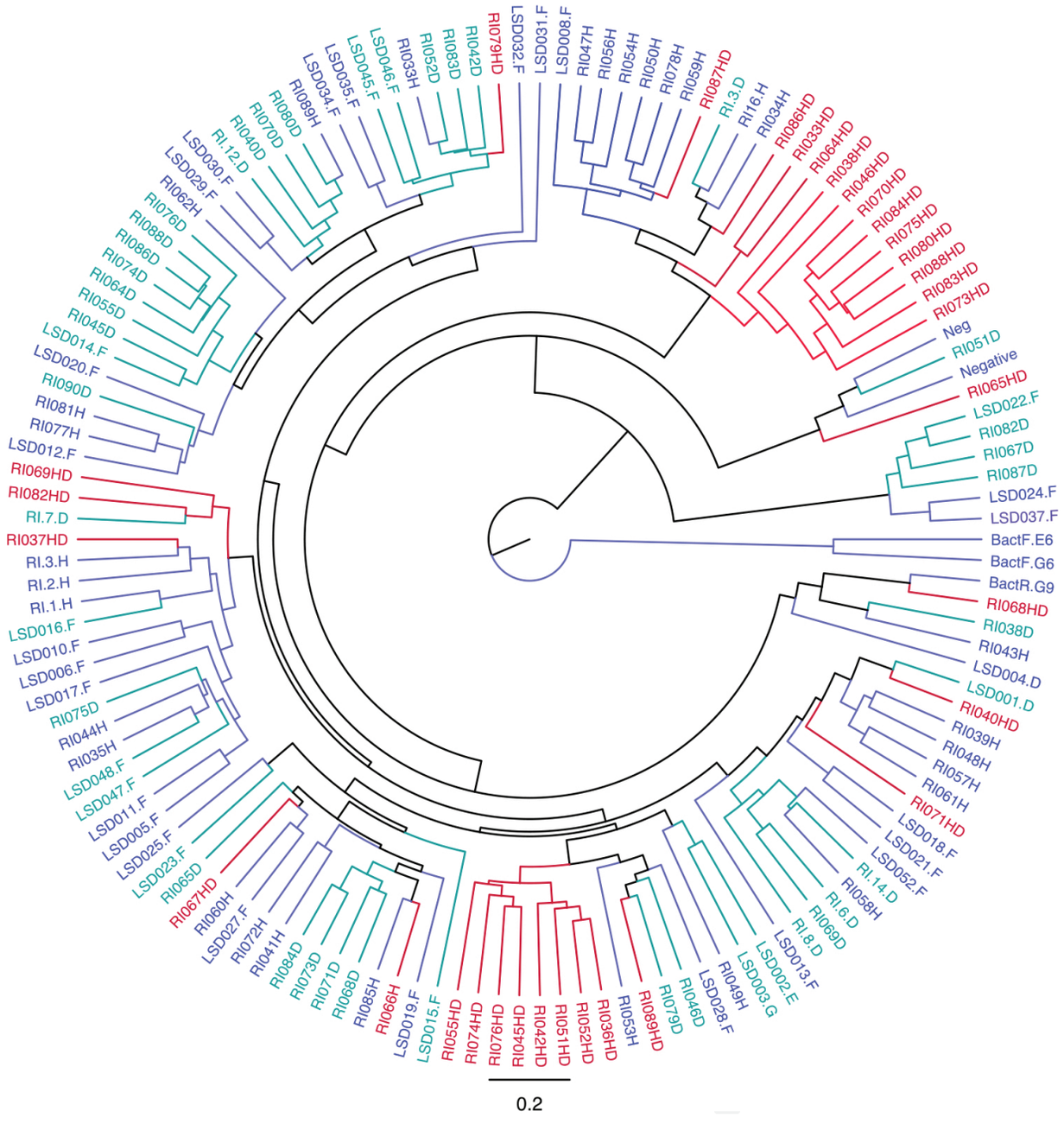

Figure 4. Weighted UniFrac tree. The disease classes are color coded. Healthy samples are blue (n = 47), diseased samples are green (n = 55), and healthy-on-diseased samples are red (n = 33).

Figure 5 is a principal coordinate analysis (PCO) of the normalized abundances of the genera identified in each disease class using a Bray-Curtis distance metric. The PCO performs an Eigen analysis that clusters the data based on the variance of all features (genera) of the data matrix [33]. One can see a clustering of the Diseased samples (red dots) that is somewhat distinct from the Healthy (yellow) and Healthy-on-Diseased (blue) samples.

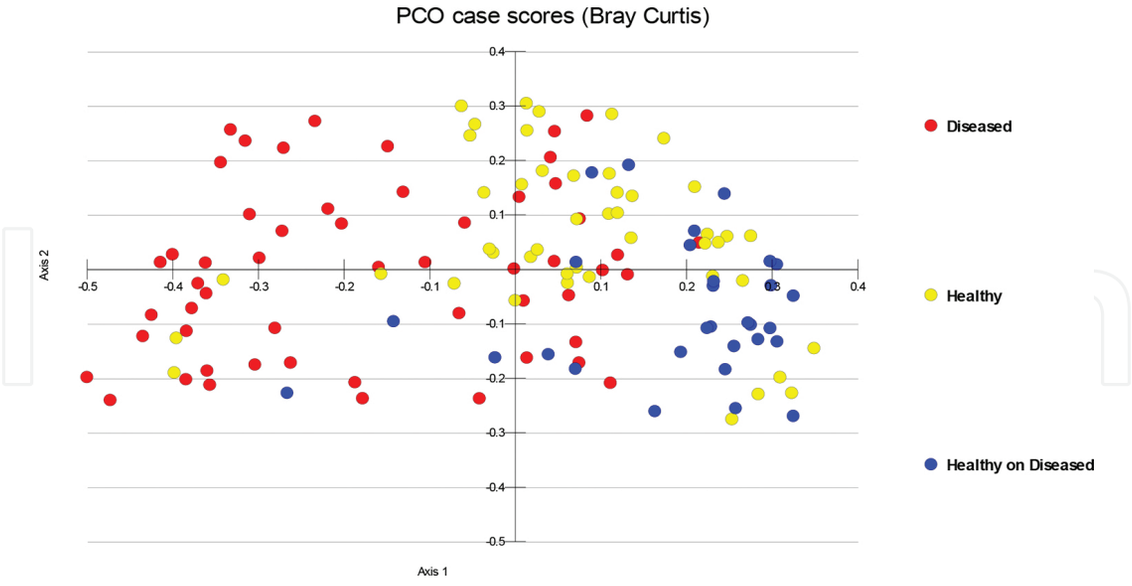

Figure 5. PCO of the normalized abundances of the genera from each disease class. The Healthy samples are yellow dots (n = 47), the Diseased samples are red dots (n = 55), and the Healthy-on-Diseased samples are blue dots (n = 33).

3.3. DA

The DA for the first comparison, the bacterial taxa on cuticle from Diseased versus apparently Healthy lobsters, included a tolerance test that eliminated 112 variables because they lacked variance between groups and thus did not significantly contribute to the discriminant function. Thus, the analysis between the two groups relied on 58 variables. The functions at the group centroids were 1.463 for disease class 1 (Diseased) and -1.1712 for disease class 2 (Healthy). The group centroids are a central measure of a set of multivariate data similar to the mean in univariate analyses. These scores demonstrate that the centroids were well separated. Such a separation between centroids demonstrates that the function is able to discriminate one class from another. The canonical correlation coefficient (R_c^2=0.848) is equivalent to the coefficient of determination (r^2) in univariate statistical analyses [35]. Wilks' λ (=0.281) is indicative of the contribution of the independent variable to the discriminant function. The lower the value of Wilks' λ is, the greater is the contribution. When Wilks' λ approaches 1, then the group means are nearly the same, and the contribution of the independent variable to the discriminant function approaches zero. The χ^2 test (χ^2=91.287; p=0.002; df=56) also indicates that the function is discriminating between classes [34]. In the second analysis (Diseased vs. Healthy-on-Diseased), the functions at group centroids were 2.060 for disease class 1 (Diseased) and -3.541 for disease class 3 (Healthy-on-Diseased). Again, these scores demonstrate that the function was discriminating between the classes (R_c^2=0.939; Wilks' λ=0.118; χ^2=131.382; p=0.000; df=47). In the third analysis (Healthy vs. Healthy-on-Diseased), the functions at group centroids were 2.439 for disease class 2 and -3.582 for disease class 3 (R_c^2=0.948; Wilks' λ=0.100; χ^2=122.991; p=0.000; df=47).

The classification results (confusion matrix) of all three analyses are displayed in **Table 1**. The confusion matrix is run as a test of the ability of the discriminant function to predict the

membership of the cases accurately. In the first analysis (Diseased vs. Healthy), the function predicted 94.1% of the original grouped cases correctly. The second analysis (Diseased vs. Healthy-on-Diseased) predicted 98.9% and the third analysis (Healthy vs. Healthy-on-Diseased) predicted 100% of original grouped cases correctly. This is further evidence that the respective functions for each of these comparisons are reliably discriminating between cases.

Classification results: Diseased vs. Healthy					
		Disease class	Predicted group membership		
			Diseased	Healthy	Total
Original	Count	Diseased	52	3	55
		Healthy	3	44	47
	%	Diseased	94.5	5.5	100.0
		Healthy	6.4	93.6	100.0
Diseased vs. Healthy-on-Diseased					
		Disease class	Predicted group membership		Total
			Diseased	Healthy-on-Diseased	
Original	Count	Diseased	54	1	55
		Healthy-on-Diseased	0	32	32
	%	Diseased	98.2	1.8	100.0
		Healthy-on-Diseased	0	100.0	100.0
Healthy vs. Healthy-on-Diseased					
		Disease class	Predicted group membership		Total
			Healthy	Healthy-on-Diseased	
Original	Count	Healthy	47	0	47
		Healthy-on-Diseased	0	32	32
	%	Healthy	100.0	0	100.0
		Healthy-on-Diseased	0	100.0	100.0

Table 1. DA confusion matrices.

Table 2 displays the standardized canonical discriminant coefficients for all three classes. These coefficients are semipartial coefficients that compare the relative importance of the variable to the independent variable. They are analogous to the β weights of regression analysis [34]. In this table, the variables with positive correlation coefficients are listed in descending order, whereas those with negative coefficients are listed in ascending order. This is done to reflect that the magnitude conveys the quantity of the correlation, and the sign indicates the quality (positive or negative). An inspection of this table reveals that only a small

number of taxa have a number higher than 1, indicating that their correlation with the disease is not strong.

Diseased vs. Healthy		**Diseased vs. Healthy-on-Diseased**		**Healthy vs. Healthy-on-Diseased**	
Taxon	**Coefficient**	**Taxon**	**Coefficient**	**Taxon**	**Coefficient**
Anaerococcus	2.769	*Anaerococcus*	1.601	*Leucothrix*	1.082
Fluoribacter	2.613	*Leucothrix*	0.805	*Fluviicola*	1.064
Alkalilimnicola	2.031	*Jannaschia*	0.786	*Burkholderia*	1.045
Crenothrix	1.745	*Corynebacterineae*	0.748	*Corynebacterineae*	1
Burkholderia	0.831	*Cellulophaga*	0.747	*Turicibacter*	0.784
Pasteuriaceae Incertae Sedis	0.691	*Filomicrobium*	0.609	*Jannaschia*	0.708
Cellulophaga	0.472	*Aquimarina*	0.552	*Cycloclasticus*	0.705
Haliscomenobacter	0.433	*Crenothrix*	0.493	Carnobacteriaceae_1	0.647
Fluviicola	0.378	*Cycloclasticus*	0.456	Alishewane	0.63
Ahrensia	0.361	Glycomycineae	0.447	*Branhamella*	0.612
Jannaschia	0.359	*Hyphomicrobium*	0.413	*Erythrobacter*	0.607
Devosia	0.349	*Alkalilimnicola*	0.297	*Frankineae*	0.597
Kangiella	0.335	*Geothermobacter*	0.297	*Frateuria*	0.479
Frateuria	0.324	*Achromobacter*	0.244	*Fluoribacter*	0.443
Hyphomicrobium	0.296	*Leisingera*	0.213	*Lactococcus*	0.429
Hirschia	0.253	*Hirschia*	0.186	*Leisingera*	0.423
Aquimarina	0.249	*Haliscomenobacter*	0.114	*Erythromicrobium*	0.347
Glycomycineae	0.192	Caldilineacea	0.113	Flexithrix	0.344
Hydrogenovibrio	0.166	*Brumimicrobium*	0.106	Glycomycineae	0.293
Lacinutrix	0.164	*Achromatium*	0.103	*Algibacter*	0.24
Branhamella	0.159	Flexithrix	0.099	*Cardiobacterium*	0.229
Aminomonas	0.155	*Geopsychrobacter*	0.021	*Aquimarina*	0.19
Brumimicrobium	0.149	*Erythrobacter*	0.015	*Kaistia*	0.157
Oceanibulbus	0.122	*Agrobacterium*	0.012	*Hydrogenovibrio*	0.097
Kaistia	0.11	*Delftia*	-1.584	*Chrysiogenes*	0.037
Caldilineacea	0.101	*Dokdonia*	-0.684	*Haliscomenobacter*	-1.52
Algibacter	0.087	*Erythromicrobium*	-0.559	*Oceanibulbus*	-0.78
Leisingera	0.087	*Kangiella*	-0.474	*Abiotrophia*	-0.73
Colwellia	0.078	*Ahrensia*	-0.423	Acidimicrobineae	-0.578

Diseased vs. Healthy		Diseased vs. Healthy-on-Diseased		Healthy vs. Healthy-on-Diseased	
Taxon	**Coefficient**	**Taxon**	**Coefficient**	**Taxon**	**Coefficient**
Kordiimonas	0.052	Carnobacteriaceae_1	-0.395	*Kangiella*	-0.531
Geopsychrobacter	0.024	Pasteuriaceae Incertae Sedis	-0.392	*Hoeflea*	-0.505
Agrobacterium	0.011	*Chrysiogenes*	-0.384	*Devosia*	-0.448
Turicibacter	0.01	*Devosia*	-0.371	*Dokdonia*	-0.348
Delftia	-3.464	*Oceanibulbus*	-0.308	*Ahrensia*	-0.341
Flexithrix	-2.637	*Algibacter*	-0.301	*Cellulophaga*	-0.257
Chromatium	-1.586	*Kaistia*	-0.255	*Hirschia*	-0.246
Hoeflea	-1.11	*Gaetbulibacter*	-0.247	*Achromobacter*	-0.235
Chrysiogenes	-1.072	*Frankineae*	-0.23	*Crenothrix*	-0.228
Gaetbulibacter	-1.015	*Kordiimonas*	-0.207	Pasteuriaceae Incertae Sedis	-0.212
Erythrobacter	-0.867	Acidimicrobineae	-0.176	*Delftia*	-0.16
Frankineae	-0.78	*Burkholderia*	-0.176	*Alkalilimnicola*	-0.144
Geothermobacter	-0.771	*Lactococcus*	-0.162	*Hyphomicrobium*	-0.124
Dokdonia	-0.452	*Fluviicola*	-0.078	*Kordiimonas*	-0.082
Carnobacteriaceae_1	-0.429	*Fluoribacter*	-0.059	*Geothermobacter*	-0.051
Corynebacterineae	-0.378	*Lacinutrix*	-0.028	*Gaetbulibacter*	-0.031
Leucothrix	-0.267	*Cardiobacterium*	-0.018	*Lacinutrix*	-0.013
Cycloclasticus	-0.194			*Aminomonas*	-0.008
Acidimicrobineae	-0.191				
Filomicrobium	-0.161				
Lactococcus	-0.15				
Erythromicrobium	-0.147				
Cardiobacterium	-0.143				
Alishewane	-0.119				
Achromobacter	-0.01				

Table 2. Standardized canonical discriminant coefficients for all three classes.

Table 3 displays the structure coefficient table. The structure coefficients are full coefficients, meaning that they are pooled as within-groups correlations between the independent variable and the standardized canonical discriminant coefficients [34]. According to Klecka [35], the structure coefficient is the authoritative coefficient for determining the importance of the independent variable to the discriminant function. As with the standardized canonical

http://dx.doi.org/10.5772/63498

discriminant coefficient, the absolute value represents the quantity and the sign indicates quality of the correlation. In the case of structure coefficients, however, the largest absolute is 1.0. If a taxon had a correlation close to +1, then it could be identified as a cause of the disease. An examination of the table reveals that *Aquimarina* spp. have a structure coefficient of 0.268, indicating that it has a weak correlation with the function. *Aquimarina* ranks second in the structure coefficient table to the genus *Jannaschia*, which has a structure coefficient of 0.325. This table has been arranged to display a descending order of importance, with the positive coefficients listed first. In the case of the negative coefficients, they appear to be listed in ascending order because the absolute value is indicative of a stronger correlation. These weak correlations indicate that there is no one pathogen that correlates definitively with the disease.

Diseased vs. Healthy		**Diseased vs. Healthy-on-Diseased**		**Healthy vs. Healthy-on-Diseased**	
Taxon	**Coefficient**	**Taxon**	**Coefficient**	**Taxon**	**Coefficient**
Jannaschia	0.325	*Jannaschia*	0.315	*Jannaschia*	0.248
Aquimarina	0.268	*Aquimarina*	0.156	*Leisingera*	0.127
Hirschia	0.173	*Cycloclasticus*	0.125	*Corynebacterineae*	0.113
Oceanicola	0.152	*Hirschia*	0.112	*Frankineae*	0.112
Methylosarcina	0.148	*Corynebacterineae*	0.076	*Leucothrix*	0.094
Schineria	0.148	*Filomicrobium*	0.073	*Cycloclasticus*	0.09
Shigella	0.143	*Cardiobacterium*	0.066	*Hirschia*	0.063
Tenacibaculum	0.142	*Leisingera*	0.059	*Kaistia*	0.062
Terasakiella	0.141	*Leucothrix*	0.055	*Aminomonas*	0.057
Filomicrobium	0.139	*Haliscomenobacter*	0.051	*Crenothrix*	0.057
Thalassobacter	0.125	*Kaistia*	0.043	*Hoeflea*	0.054
Microbulbifer	0.105	Glycomycineae	0.043	*Erythrobacter*	0.052
Photobacterium	0.104	*Burkholderia*	0.043	*Cardiobacterium*	0.048
Lacinutrix	0.099	*Frankineae*	0.04	Glycomycineae	0.045
Streptococcus	0.092	*Brumimicrobium*	0.03	*Hydrogenovibrio*	0.045
Woodsholea	0.089	*Geopsychrobacter*	0.03	*Frateuria*	0.044
Vibrio	0.073	*Agrobacterium*	0.03	*Fluviicola*	0.044
Haliscomenobacter	0.065	*Fluviicola*	0.03	*Haliscomenobacter*	0.044
Ruegeria	0.063	*Achromatium*	0.03	*Lactococcus*	0.036
Psychrobacter	0.06	Caldilineacea	0.03	*Chrysiogenes*	0.035
Roseovarius	0.058	Flexithrix	0.03	*Chromatium*	0.031
Shinella	0.058	*Alkalilimnicola*	0.03	*Branhamella*	0.031
Fluoribacter	0.058	*Chromatium*	0.03	*Alkalilimnicola*	0.031
Ralstonia	0.058	*Colwellia*	0.03	Flexithrix	0.031

Diseased vs. Healthy		Diseased vs. Healthy-on-Diseased		Healthy vs. Healthy-on-Diseased	
Taxon	**Coefficient**	**Taxon**	**Coefficient**	**Taxon**	**Coefficient**
Carnobacteriaceae_2	0.058	*Anaerococcus*	0.03	Alishewane	0.031
Curvibacter	0.058	*Hoeflea*	0.03	*Burkholderia*	0.031
Schlegelella	0.058	*Delftia*	0.025	*Turicibacter*	0.031
Diaphorobacter	0.058	*Hyphomicrobium*	0.025	Carnobacteriaceae_1	0.019
Pseudomonas	0.058	*Ahrensia*	0.023	*Ahrensia*	0.013
Asticcacaulis	0.058	*Lactococcus*	0.021	Acidimicrobineae	0.011
Stenotrophomonas	0.058	*Lacinutrix*	0.019	*Delftia*	0.007
Staphylococcus	0.058	*Crenothrix*	0.015	*Algibacter*	0.004
Colwellia	0.058	*Dokdonia*	0.001	*Aquimarina*	-0.002
Methylobacterium	0.058	*Achromobacter*	-0.274	*Abiotrophia*	-0.004
Hyphomicrobium	0.058	*Cellulophaga*	-0.191	*Dokdonia*	--0.016
Achromatium	0.058	*Chrysiogenes*	-0.131	*Achromobacter*	-0.018
Geopsychrobacter	0.058	*Abiotrophia*	-0.116	*Cellulophaga*	-0.046
Brumimicrobium	0.058	*Fluoribacter*	-0.115	*Hyphomicrobium*	-0.046
Spirochaeta	0.058	*Erythrobacter*	-0.109	*Lacinutrix*	-0.046
Caldilineacea	0.058	*Algibacter*	-0.091	*Erythromicrobium*	-0.063
Agrobacterium	0.058	*Hydrogenovibrio*	-0.079	*Fluoribacter*	-0.066
Cellulophaga	0.058	Carnobacteriaceae_1	-0.068	*Gaetbulibacter*	-0.069
Anaerococcus	0.058	Acidimicrobineae	-0.052	*Geothermobacter*	-0.072
Roseobacter	0.049	*Erythromicrobium*	-0.052	*Oceanibulbus*	-0.09
Nereida	-0.263	*Geothermobacter*	-0.046	*Kordiimonas*	-0.103
Glycomycineae	-0.236	*Oceanibulbus*	-0.042	*Devosia*	-0.118
Silicibacter	-0.206	*Kordiimonas*	-0.037	Pasteuriaceae Incertae Sedis	-0.169
Stappia	-0.179	*Gaetbulibacter*	-0.015	*Kangiella*	-0.258
Cycloclasticus	-0.177	*Devosia*	-0.013		
Sulfitobacter	-0.175	Pasteuriaceae Incertae Sedis	-0.013		
Phaeobacter	-0.173	*Kangiella*	-0.004		
Cloacibacterium	-0.172				
Erythromicrobium	-0.165				
Salinibacter	-0.153				
Carnobacteriaceae_1	-0.15				

http://dx.doi.org/10.5772/63498

Diseased vs. Healthy		Diseased vs. Healthy-on-Diseased		Healthy vs. Healthy-on-Diseased	
Taxon	**Coefficient**	**Taxon**	**Coefficient**	**Taxon**	**Coefficient**
Branhamella	-0.143				
Turicibacter	-0.141				
Leadbetterella	-0.132				
Geothermobacter	-0.124				
Alishewane	-0.12				
Hyphomonas	-0.115				
Nannocystaceae	-0.113				
Comamonas	-0.11				
Algibacter	-0.11				
Piscirickettsia	-0.11				
Fluviicola	-0.101				
Propionibacterineae	-0.099				
Chrysiogenes	-0.099				
Gp4	-0.096				
Crenothrix	-0.095				
Leucothrix	-0.095				
Methylocapsa	-0.094				
Krokinobacter	-0.092				
Frateuria	-0.09				
Zobellia	-0.088				
Sphingomonas	-0.088				
Rubellimicrobium	-0.086				
Kaistia	-0.083				
Maribacter	-0.081				
Gaetbulibacter	-0.078				
Hoeflea	-0.068				
Hydrogenovibrio	-0.068				
Acidimicrobineae	-0.068				
Saccharophagus	-0.068				
Meganema	-0.068				
Aminomonas	-0.068				
Nitrospira	-0.068				
Thiorhodospira	-0.068				

Diseased vs. Healthy		Diseased vs. Healthy-on-Diseased		Healthy vs. Healthy-on-Diseased	
Taxon	**Coefficient**	**Taxon**	**Coefficient**	**Taxon**	**Coefficient**
Thioclava	-0.068				
Rhodomicrobium	-0.068				
Sphingopyxis	-0.068				
Pibocella	-0.068				
Winogradskyella	-0.068				
Rhodobaca	-0.063				
Nitrosospira	-0.063				
Microvirga	-0.06				
Erythrobacter	-0.06				
Corynebacterineae	-0.059				
Frankineae	-0.051				
Micrococcineae	-0.05				

Table 3. Structure coefficient table.

For the second comparison of the bacterial taxa on the cuticle of Diseased lobsters versus Healthy cuticle on Diseased lobsters, the functions at the group centroids were well separated with a value of 2.060 for disease class 1 (Diseased) and -3.541 for disease class 3 (Healthy-on-Diseased; R_c^2=0.939; Wilks' λ=0.118; χ^2=131.382; p<0.001; df=47). As in the first comparison, these data indicate that the function is discriminating between the classes.

Jannaschia spp. appears to have roughly the same structure coefficient as in the previous analysis (0.315). *Aquimarina* spp. has a structure coefficient of 0.156.

Although these are the taxa with the highest positive structure coefficients, they are considerably less than 1. This indicates that, although they do discriminate for the disease compared to Healthy-on-Diseased samples, they do so weakly. *Aquimarina* spp. discriminated more weakly between Diseased and Healthy-on-Diseased classes than between Diseased and Healthy classes. This might indicate that, as a Healthy lobster converts to a Diseased lobster, the abundance of *Aquimarina* spp. increases. There would be more of these bacteria present on the unblemished surface of a lobster with ESD compared to Healthy lobsters but still less than in the lesions.

For the third comparison of the bacterial taxa on the cuticle of Healthy lobsters versus Healthy cuticle on Diseased lobsters, the discriminant functions at the group centroids demonstrated a good separation with values of 2.439 for disease class 2 (Healthy) and -3.582 for disease class 3 (Healthy-on-Diseased; R_c^2= 0.948; Wilks' λ=0.100; χ^2=122.991; p<0.001; df=47). In this analysis, *Aquimarina* spp. have a structure coefficient of -0.002, which indicates that it correlates weakly and negatively in discriminating between carapace from lobsters that show no

signs of the disease and carapace samples without lesions that are taken from lobsters that have the disease.

3.4. Correlational network analysis

Figure 6 is the network diagram of bacteria from the lobsters identified as Diseased. The edges (connecting links) between the nodes (taxa) are either red (negative correlation) or blue (positive). The width of the edge corresponds to the magnitude of the correlation coefficient. An inspection of the map reveals that the genera *Aquimarina* and *Jannaschia* are negatively correlated with several other taxa. *Jannaschia* is positively correlated with *Thalassobacter* and *Thalassobius* and, by extension, is negatively correlated with *Cardiobacterium*. *Jannaschia* is also negatively correlated with *Uvibacter*, *Pibocella*, and *Leucothrix*. *Aquimarina* is also negatively correlated with *Leucothrix* as well as with *Loktanella* and *Micrococcineae*.

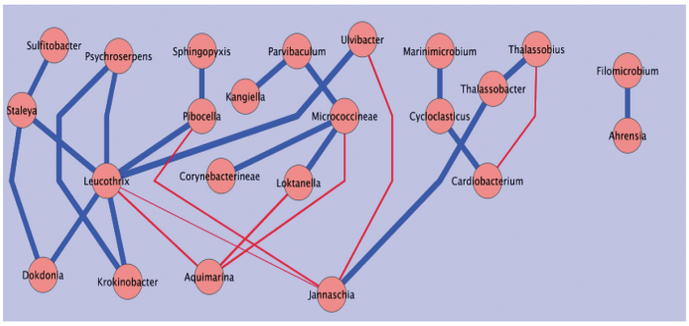

Figure 6. Correlational network map of the Diseased microbiome.

Figure 7 is the network diagram of bacteria from the lobsters identified as Healthy. In this diagram, *Corynebacterineae* appear to occupy a central point that connects most of the nodes and is negatively correlated with *Cycloclasticus* and *Cardiobacterium* but positively correlated with *Maribacter*, *Propionibacterineae*, *Frankineae*, and *Micrococcineae*. *Cardiobacterium* also appears to occupy a hub-like position and is negatively correlated with *Micrococcineae* and positively correlated with *Cycloclasticus* and *Psychroserpens*. There is a secondary cluster that is disconnected from the larger one. In this disconnected cluster, *Ahrensia* occupies a central position between *Erythrobacter*, *Sphingocinella*, and *Parvibaculum*. *Erythrobacter* and *Parvibaculum* are also linked to form a clique with *Ahrensia*, and *Erythrobacter* is also linked to *Sphingopyxis*, which in turn is linked to *Rubellimicrobium*. All of these taxa are positively correlated with one another. There are also three unconnected dyads. *Leucothrix* is associated with *Crenothrix*, *Thalassobacter* is associated with *Nereida*, and *Ulvibacter* is associated with *Marinimicrobium*. The pairs in all three dyads are positively correlated with one another.

Figure 8 represents the Healthy-on-Diseased microbiome correlations. In this map, there are five unconnected clusters. The largest consists of four taxa in which all are positively correlated. The connection is an unbranched chain with *Micrococcineae*, *Marinimicrobium*, *Algibacter*, and *Cycloclasticus* in sequence. There are two triads that do not form a complete clique. *Ulvibacter*, *Rubellimicrobium*, and *Ahrensia* are all positively correlated. In the second triad,

Cardiobacterium is negatively correlated with *Leucothrix*, which is positively correlated with *Nitratireductor*. There are two dyads in which all taxa are positively correlated: *Thalassobius* and *Loktanella* form one and *Krokinobacter* and *Piscrikettsia* form the second.

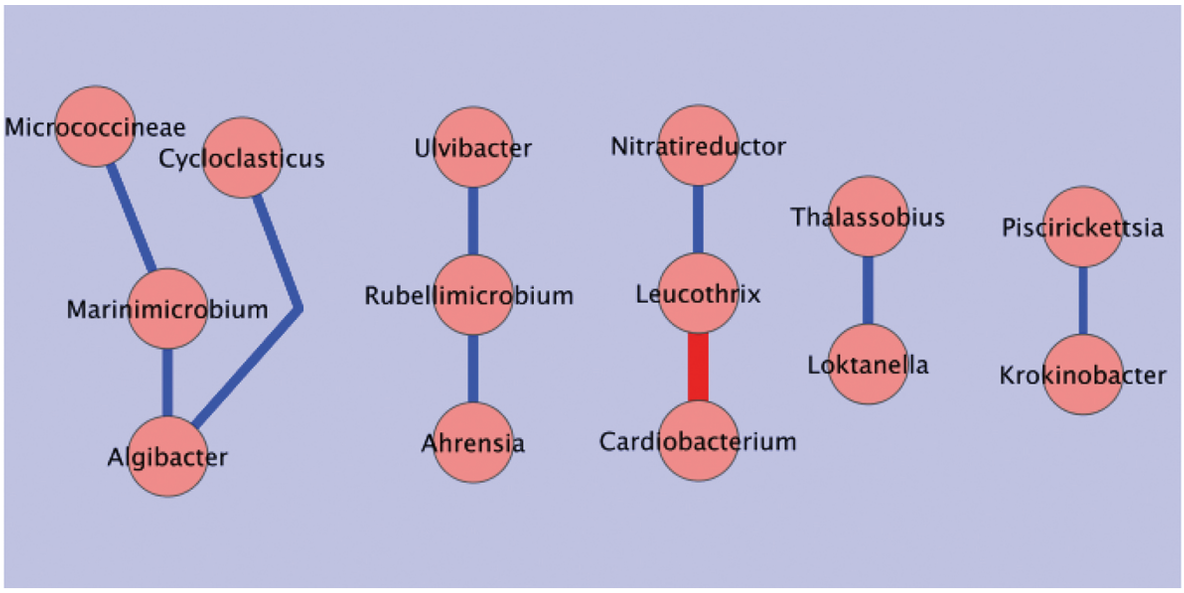

Figure 8. Correlational network map of the Healthy-on-Diseased microbiome.

Comparing the three maps, the average clustering coefficient of the Diseased microbiome is 0.289, the Healthy microbiome has an average clustering coefficient of 0.337, and the Healthy-on-Diseased microbiome has an average clustering coefficient of 0.0. Clustering coefficients are the ratios of the actual number of connections in comparison to the total possible connec-

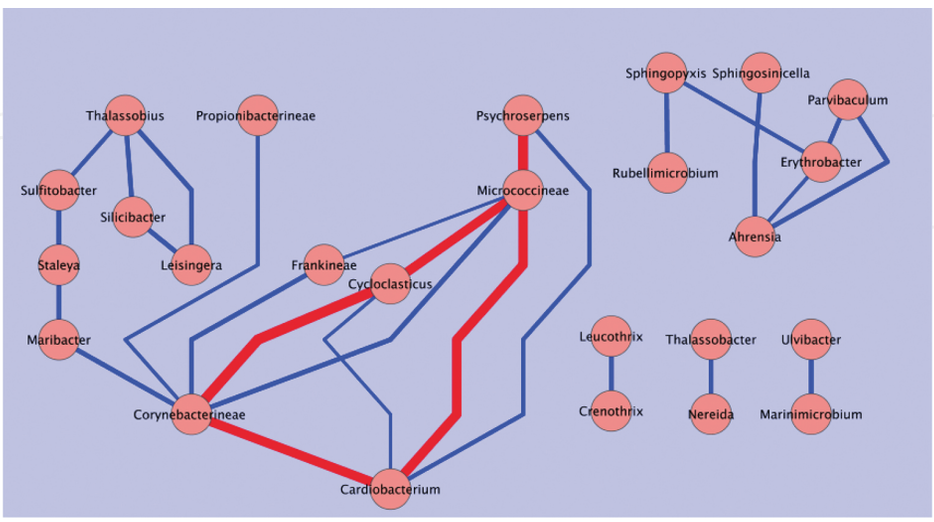

Figure 7. Correlational network map of the Healthy microbiome.

http://dx.doi.org/10.5772/63498

tions and range from 0 to 1 [41]. In other words, the clustering coefficient is the probability that one node is connected to another.

Figure 9 is a correlational difference network diagram that compares Healthy and Diseased microbiomes. This map displays taxa whose correlation coefficient changes significantly from Healthy to Diseased class. They are color coded to reflect the nature of the change. Red edge color indicates that the taxa correlate positively with the Healthy state and negatively with the Diseased state. Blue indicates that they correlate with both states positively but have a larger positive correlation coefficient in the Healthy state. Green indicates a negative correlation with both states but a larger negative correlation coefficient with the Healthy state.

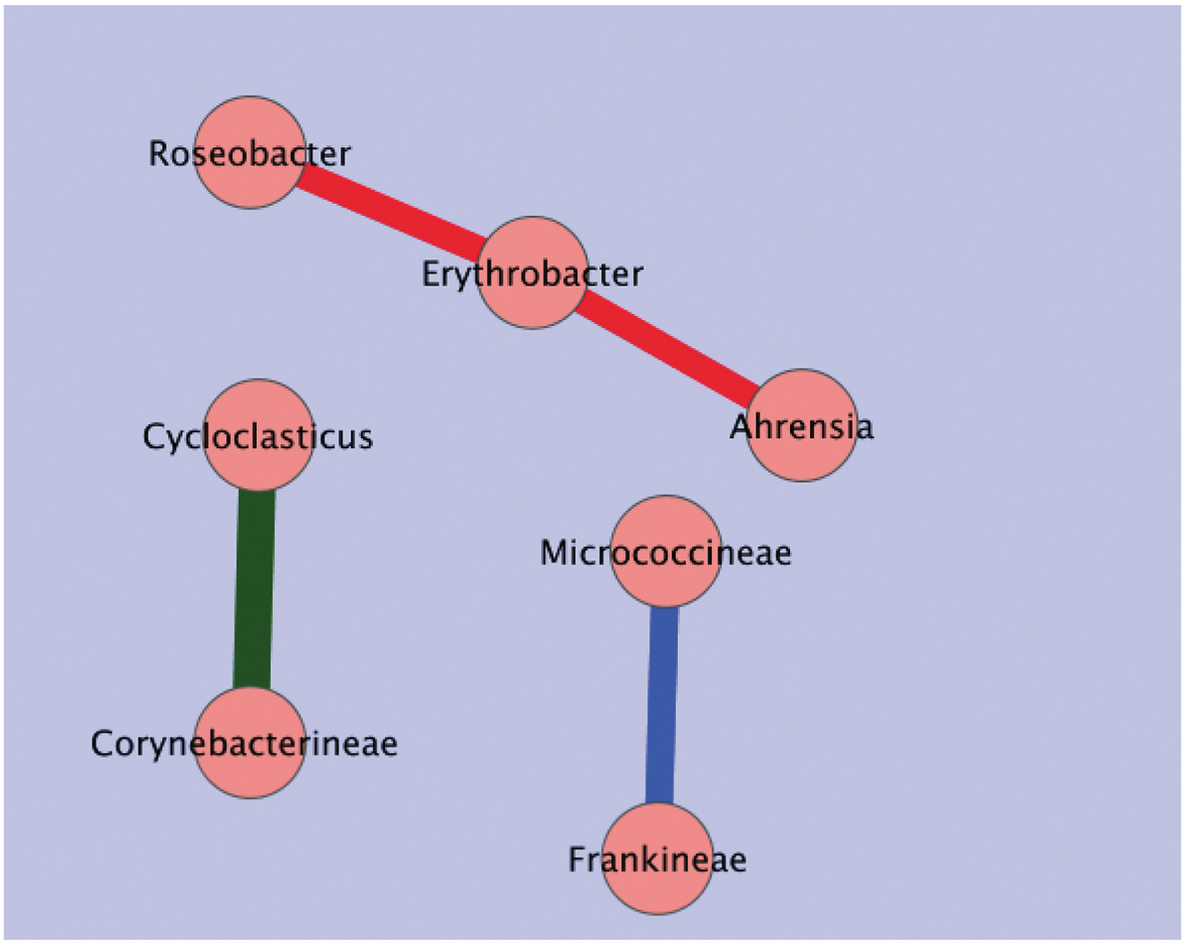

Figure 9. Correlational difference map of the Healthy versus Diseased microbiomes.

The network consists of three disconnected groups of taxa. *Ahrensia*, *Erythrobacter*, and *Roseobacter* are connected in one group. *Erythrobacter* bridges this triad, and they all are positively correlated to the Healthy state and negatively correlated to the Diseased state. *Frankineae* and *Micrococcineae* form a dyad that has a higher positive correlation with the

Healthy state than the Diseased state. *Cycloclasticus* and *Corynebacterineae* form the second dyad that correlates negatively with both states but more negatively with the Healthy state. Neither *Aquimarina* nor *Jannaschia* appears in this correlation difference network, suggesting that the observed correlation between these two taxa in the Diseased state (**Figure 6**) was not statistically different from the Healthy state. Correlational difference maps illustrate differences in the microbial community when comparing one state (disease class) to another. If there is no significant difference in the correlations between taxa when one state is compared to the other, then those taxa will not be visible on the diagram.

Figure 10 is a correlational difference diagram that compares Healthy-on-Diseased to Diseased microbiomes. The color coding is the same as **Figure 9**.

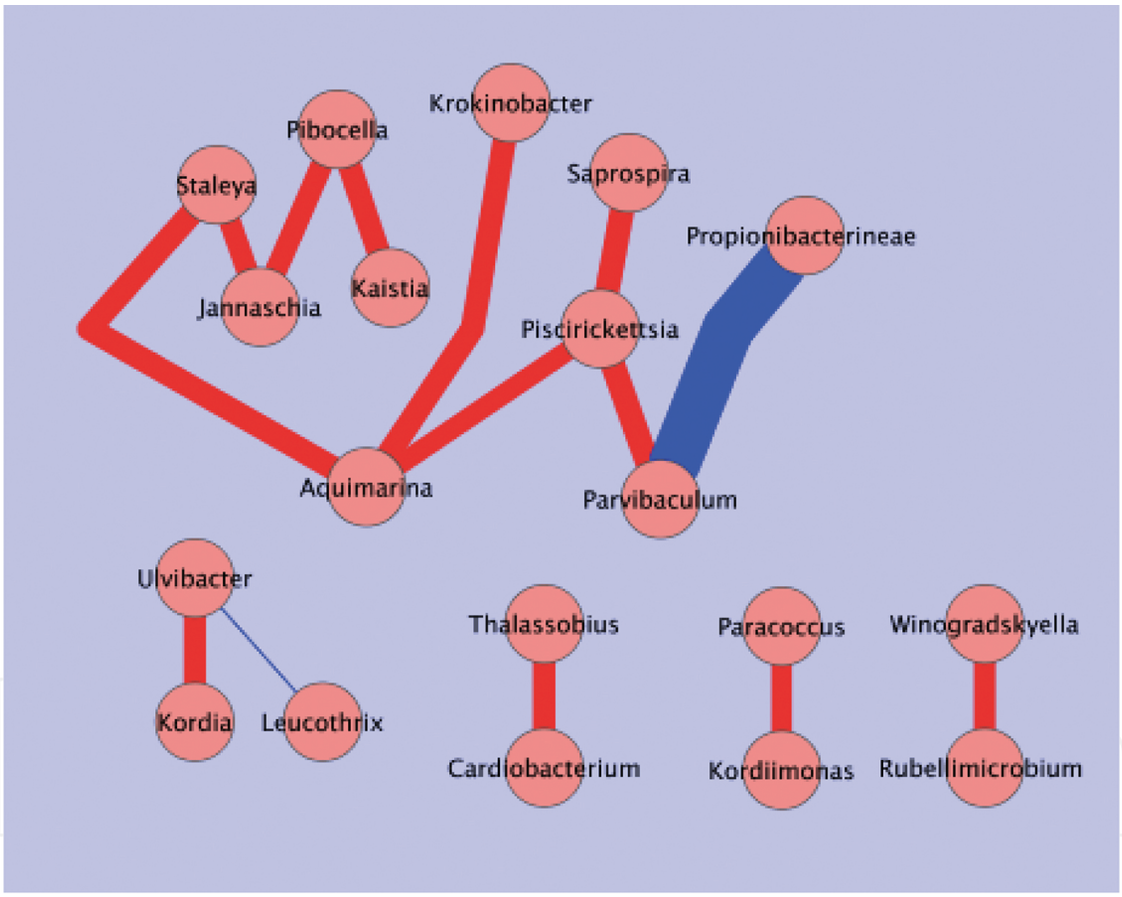

Figure 10. Correlational difference map of the Healthy-on-Diseased versus Diseased microbiomes.

This network is more complex, with a large group consisting of 10 taxa, 3 dyads, and 1 triad, suggesting that a number of potentially pathogenic processes or interactions are different in the Healthy-on-Diseased biofilm that do not occur in the Healthy biofilm. Within the large group, *Aquimarina* is connected to three taxa: *Staleya*, *Krokinobacter*, and *Piscirickettsia*. Following the first branch, *Staleya* is connected to *Jannaschia*, which is connected to *Pibocella*

and *Kaistia* in a linear fashion. *Krokinobacter* is a terminal end of its branch, and *Piscirickettsia* connects to two taxa: *Saprospira* and *Parvibaculum*. To this point, the edge color of this group is red, indicating that all are positively correlated with the Healthy-on-Diseased state and negatively with the Diseased state. *Parvibaculum* connects to *Propionibacterineae* with a blue-colored edge, indicating that this edge-node combination correlates positively more positively with Healthy-on-Diseased than with Diseased.

The triad, similar to the triad in the Healthy versus Diseased correlational difference map, forms an incomplete clique [37], with *Ulvibacter* bridging between *Kordia* and *Leucothrix*. Between *Ulvibacter* and *Kordia*, the red edge color reveals that they correlate positively with the Healthy-on-Diseased state but negatively with the Diseased state. The second edge of the triad, however, between *Ulvibacter* and *Leucothrix*, is colored blue. The three dyads have red edge colors. They consist of the pairs *Thassobius* and *Cardiobacerium*, *Paracoccus* and *Kordimonas*, and *Windgradskyella* and *Rubellimicrobium*.

4. Discussion and conclusion

Smolowitz et al. [3] found that, although more advanced cases of ESD presented with extensive lesions throughout the dorsal surface, most cases were restricted to the cephalothorax.

The bacterial diversity as measured by the Shannon index appears to be roughly similar on all regions, with the claw and cephalothorax regions having the most similar indices (see **Figure 1**). Smolowitz et al.'s observations that ESD lesions were more prevalent on the upper cephalothorax, however, influenced the decision that a further molecular study would be focused on this region of the carapace. Furthermore, as the taxa distribution is relatively similar in all regions, we would be unlikely to miss key taxa by focusing on the cephalothorax.

As mentioned previously, the inset histogram (**Figure 2**) represents 170 taxa that were identified and at a normalized abundance greater than 1%. The most abundant taxa include the genera *Jannaschia*, *Aquimarina*, *Cardiobacterium*, *Thalassobius*, and *Loktanella* and the suborder *Micrococcineae*.

Jannaschia are characterized as rod-shaped, nonmotile, Gram-negative, catalase-positive, strict aerobes that do not reduce nitrate to nitrite and found to use a wide variety of carbon sources but not chitin. Their growth appears to be restricted to seawater and cannot be cultured in the absence of seasalts [42].

Aquimarina are described as rod-shaped bacteria that possess gliding motility. They are Gram-negative, catalase-positive, strict aerobes and are capable of degrading chitin. They are also known to produce various flexirubin and carotenoid pigments. Similar to *Jannaschia*, *Aquimarina* appear to be dependent on seawater to grow [43].

Cardiobacterium are described exclusively in the literature as human pathogens implicated in endocarditis and peritonitis. They are also found as normal constituents in human nasal and oral cavity microflora. They are catalase-negative, Gram-negative pleomorphic bacilli. They

are facultative anaerobes that ferment carbohydrates but do not reduce nitrate to nitrite. Although implicated in serious infections, members of this genus are not exceptionally virulent (a large inoculate is necessary to initiate an infection) [44].

Thalassobius are Gram-negative, strict aerobes that do not produce pigments and tend to favor organic acids as a carbon and energy source rather than carbohydrates. Some members of the genus exhibit motility; others do not [45].

Loktanella are Gram-negative, strict aerobes that do not use carbohydrates but can degrade urea, Tween 80, citrate, and aesculin [46].

The suborder *Micrococcineae* includes 15 families that collectively include more than 90 genera as well as 4 genera that have not been classified as members of a family. This group is a metabolically diverse, Gram-positive taxon [47]. What this specific OTU represents is unclear from these data.

These taxa do conform, however, to what has been observed about ESD. There is some, but not extensive, degradation of chitin. In these six genera, only one genus (*Aquimarina*) is observed to be chitinovorous. As mentioned above, there is high lipase activity in lesions [14], and lipids appear to be the preferential carbon and energy source of *Loktanella*. There are generalists in the group, such as *Jannaschia*, and there are those that use organic acids, including amino acids (*Thalassobius*). The presence of a fermenter, such as *Cardiobacterium*, could indicate that anaerobic conditions develop concomitantly with the progression of the lesions.

Bell et al. [14] found that ectohydrolase activity differed within the biofilms of lobsters from the geographic areas with high ESD incidence compared to lobsters inhabiting areas of little to no ESD. This could indicate that there is a shift in metabolic activity of the bacteria that are present or could indicate a shift in population.

The neighbor joining tree (**Figure 3**) of *Aquimarina* species reveals that the genus is present in all samples. There is no emergent pattern of members of the genus that correlates with either state of health. These data suggest that members of the genus *Aquimarina* are ubiquitous but do not eliminate them as opportunists if there is an underlying susceptibility in the lobster. This supports the dysbiosis model of ESD. A discrete pathogenic microorganism does not cause the disease; rather, the bacterial infection is the result of a change in the biofilm, either in community structure or in metabolic activity, which could have a different underlying cause. Laufer et al. [16], as explained in Section 1, found that lobsters with ESD had higher tissue concentrations of alkylphenols than did lobsters that did not present with the disease. Other studies of the same lobsters used in this study also found a higher incidence of idiopathic ailments such as hepatopancreatitis and ocular lesions in Rhode Island lobsters compared to their Maine counterparts [15], and other researchers found differences in bacterial ectohydrolase activity on the surface of lobsters from these distinct regions [14]. This suggests that there may be environmental conditions present in Rhode Island waters that are causing the native lobsters to be more susceptible to disease.

Researchers have implicated a novel species (*A. homaria*) in the initiation of a laboratory-induced form of shell disease [12]. The author's investigation found no evidence of this specific

http://dx.doi.org/10.5772/63498

species in any of the samples, although we did find related species. Furthermore, the induced shell disease studied here does not conform to the histological profile that has been described for ESD [12].

An inspection of the UniFrac data that are depicted by the tree (**Figure 4**) reveals that, although there is some clustering, the lobsters identified as Healthy and Diseased show enough similarity that they exist as neighbors on all of the major branches of the tree. There is no statistically significant difference between the three classes as demonstrated by the enumeration of their *p* values. Again, this supports the hypothesis that this disease is not caused by a discrete pathogen.

The PCO reveals much the same pattern; although there are identifiable regions, there is an overlap between the classes.

Our original simple hypothesis is that there is a significant difference between the bacterial communities in the Healthy and Disease states, indicating that this difference is associated with the etiology of the disease. The null hypothesis asserts that the bacterial communities are similar on the Healthy and Diseased lobsters. The phylogenetic metrics employed to compare the microbiomes of subjects in this study indicate that there is no significant difference between the three classes, which leads us to accept the null hypothesis and reject the original hypothesis. However, these data suggest that, although there may not be a gross difference between the microbiomes of Healthy and Diseased lobsters, there is a subtle shift that requires further investigation and the definition of a more complex hypothesis. A major avenue of inquiry would be to determine whether this shift is one of the metabolic activities among essentially the same bacteria, if there is an emergence of some members of the population that displace other extant members, or if there are new recruits to the community from outside the biofilm. Wahl et al. [48] suggested the use of emergent techniques, such as desorption electrospray ionization-mass spectrometry, as a means of surveying the surface of the biofilm to elucidate the metabolic compounds that are present in biofilms. Coupled with confocal microscopy techniques, as suggested by Costerton [24], researchers could begin to develop a spatial representation of the lobster surface microbiome that would include both the identity of the bacterial cells and the metabolic activity that was occurring in their vicinity.

From the perspective of disease etiology, this kind of shift may point to a cause other than bacterial. If the same microflora, albeit in different abundances, are found on lobsters that have the disease as well as on those that are apparently healthy, then perhaps this dysbiosis represents a sign of some kind of disorder that is caused by something other than bacteria. Laufer et al. [16] established a correlation between lobsters with ESD and high tissue concentrations of alkylphenols. As noted earlier, these compounds retard the cross-linking of tyrosine moieties in the carapace, which makes shell hardening take longer. Tarrant et al. [21] found evidence to suggest that gene expression in lobsters affected by ESD might indicate increased exposure to xenobiotics. Homerding et al. [20] found that lobsters living in the geographic area with a high incidence of ESD presented with reduced immunocompetence. This evidence supports an assertion that ESD is not primarily a bacterial disease but that bacterial lesions are a manifestation of a systemic dysfunction.

Kunkel et al. [10] discovered that lobsters with ESD had a loss of calcification in and around the disease lesions, particularly in the trabecular structures that are composed of apatite. One question that needs to be investigated further is whether the decalcification is related to the presence of alkylphenols. Could exposure of the underlying structure to the environment lead to decalcification? Alternatively, could acidic metabolic products of bacterial action produce the same results?

To use an analogy, suppose there is a house whose roof is defective. Imagine the nails were weak and could not hold the protective components of the roof in place, similar to the protein-chitin structures in the lobster carapace in which the tyrosine cross-linking was not complete. Rainwater would leak into the underlying structure, analogous to seawater getting into the trabecular apatite of the lobster carapace. In both cases, this would physically weaken the underlying structure. In both cases, normal microflora would have access to parts of the structure from which they would normally be excluded and may start to use these energy and carbon sources. This would further weaken and disfigure the structure and increase the likelihood of a breach in the outer protective structure. In this analogy, it is not the microflora that causes the problem in the roof. Rather, the rot that would ensue from its invasion is the result of the ineffectiveness of barriers whose function is to keep these organisms out of the underlying structure. In the case of ESD, perhaps the bacterial lesions are not the cause of the disease but merely the inevitable result of structural weaknesses in the lobster carapace. Additionally, the trabecular apatite and the other calcium moieties present in the lobster cuticle may have antimicrobial properties themselves [10]. Their physical dissolution could be the result of the intrusion of acidified seawater, as there is now evidence that ocean acidification is affecting organisms that produce calcareous shells [49]. The absence calcium moieties from the site of lesions could represent an additional reduction in the ability to exclude microbiota from the exoskeleton.

Although there have been other studies of biofilms related to crustaceans [50, 51], this represents the first survey of the surface microbiome of the lobster that uses high-throughput, culture-independent molecular techniques. As mentioned above, it is by no means an exhaustive analysis of the lobster microbiome, as the subjects of this study are geographically restricted and are not a large enough size to yield a global generalization. It is comprehensive enough, however, to demonstrate that, although there is no gross difference between the microbiomes of lobsters with and without ESD in Rhode Island samples, there may be a subtle shift in the microbial population that correlates with dysfunction. As mentioned previously, Bell et al.'s work indicates a variance in the metabolic activity of bacteria in eastern Long Island Sound, an area of high ESD occurrence, compared to those found on the surface of lobsters in regions that have little to no ESD incidence [14]. This shift may be more closely related to a shift in activity rather than of population.

Considering the first DA analysis (Diseased vs. Healthy), the canonical correlation coefficient (R_c^2) value of 0.848 indicates a high correlation of the discriminant function and the groups [34]. The second and third analyses have lower values. This indicates that the 58 bacteria that were retained after the initial tolerance test are useful in discriminating between disease classes. Presumably, the 112 bacteria that were rejected because their abundan-

http://dx.doi.org/10.5772/63498

ces are similar in both classes are not contributing to the disease state. The structure matrix indicates that the genus *Aquimarina* is weakly correlated with the Diseased state. Its structure coefficient is second only to the genus *Jannaschia*.

This analysis supports the affirmative hypothesis that there is a difference between the microbial taxa in shell-diseased lobsters compared to healthy lobsters. The study identifies 58 bacteria that are significantly different between the two classes and rejects 112 that do not contribute to discrimination between them. The relatively low correlation coefficients for these 58 taxa, however, do indicate that they are present on all three classes but in slightly different abundances.

This analysis also provides additional evidence that ESD in the American lobster correlates with dysbiosis rather than the presence of a single overt pathogen. In a disease caused by a single pathogen, one would expect a structure coefficient of one of the variables to approach 1. An inspection of the structure coefficients reveals that none of the bacterial taxa have a coefficient greater than 0.325.

The role of *Aquimarina* spp. in the disease lesions is unclear. In the DA that compared the bacteria on cuticle from Diseased animals to Healthy cuticle from Diseased animals, *Aquimarina* spp. had a smaller structure coefficient (0.156) than that on Diseased versus apparently Healthy animals (0.268). One possible interpretation is that, if *Aquimarina* spp. were present at the initiation of the disease, then it should be strongly negatively correlated with the Diseased cuticle bacteria. Instead, the genus correlates weakly and positively, indicating that it discriminates the Diseased state more strongly than the pre-Diseased state. Moreover, in the analysis of taxa from Healthy lobsters versus Healthy cuticle on Diseased lobsters, the structure coefficient of *Aquimarina* spp. was negative and the lowest value of all the structure coefficients in the structure coefficient table. This indicates a weakly negative correlation. If this bacterial taxon was definitive in the initiation of the disease, a more likely scenario would be that it would correlate strongly with the unaffected surface of a Diseased lobster and would therefore have a more negative coefficient compared to the surface of Healthy lobsters.

This analysis supports the observations that were articulated above. The weak correlations of some of the taxa with the three states of health reinforce the assertion that, although there are differences in the abundances of these taxa when comparing these three states, none of them are exclusive to one or the other state. The weak correlations also demonstrate that this is not a disease caused by a discrete pathogen, which would have a much stronger correlation. The works of the author's colleagues within the New England Lobster Health Initiative strongly suggest that there are underlying causes that render some lobsters, particularly within the waters of eastern Long Island Sound and Rhode Island, susceptible to an opportunistic infection [10, 14–16, 21]. Exposure to abnormally high levels of endocrine-disrupting compounds such as alkylphenols appears to fit the profile of intervening agents, which is described by Laufer et al. and Tarrant et al.; not only are they capable of eliciting a response consistent with an endocrine-disrupting compound, but they also appear to retard proper shell development. Hitherto, there is a correlation, but no direct evidence, linking alkylphenol exposure to ESD. Obtaining such evidence would require an experiment in which a group of lobsters was exposed to alkylphenols, whereas a control group would be kept in an alkylphe-

nol-free environment. As discussed previously, however, captive lobsters are more susceptible to impoundment shell diseases [5]. Designing an experiment that would mitigate such confounding results is likely to prove challenging.

The abundance tables, as well as the DA computations reported in the previous chapter, reveal that *Aquimarina* and *Jannaschia* are more abundant (and correlate positively in DA) when the Diseased and Healthy states are compared. An inspection of the correlation network of the Diseased microbiome indicates that these two genera are negatively correlated with several of the other taxa present, indicating that, although these two are more abundant in the Diseased state, most of the others are reduced in abundance, with the exception of *Thalassobacter* and *Thalassobius*, which are positively correlated with *Jannaschia*. The average clustering coefficient for the Diseased microbiome was 0.289. For the Healthy microbiome, the coefficient was 0.337. Both of these are well below 1; therefore, neither network demonstrates a great deal of connectivity or interaction between members of the community. With a difference in the coefficients of less than 0.05, the difference between the two is negligible. In the Healthy-on-Diseased microbiome, the average clustering coefficient is 0.0, indicating that the associations between the taxa are essentially random.

The correlational difference networks may shed some light on the role of *Aquimarina* and, for that matter, *Jannaschia*. Neither can be found in the correlational difference network map that compared Healthy and Diseased lobsters. In the comparison of Healthy-on-Diseased to Diseased, however, both appear as taxa that correlate positively with the Healthy-on-Diseased state but negatively with the Diseased state. This may indicate that both are early opportunists in the lesion formation and there is a shift in their function when they move to the Diseased state.

The only data used in these correlational networks were those derived from MTPS of sample lobsters from the "100 Lobsters" Project [28]. As described in Section 1, samples from these lobsters were used in other investigations, and the data obtained have been recorded [14, 16, 20]. Integrating these data by means of correlational network analysis with alkylphenol concentrations in the tissues and ectohydrolases on the surface of the same lobster, for example, may produce a more definitive correlation between ESD and alkylphenols and may allow researchers to correlate which bacterial taxa are involved in what metabolic activity.

When comparing the data obtained using previous methods, a slightly different picture emerges. Taxa such as *Aquimarina* and *Jannaschia* appear to correlate with ESD, albeit weakly. In the DA analysis, they serve as reliable factors in discriminating cases of the disease. They appear, however, to have somewhat weaker interactions with other constituents of the biofilm as demonstrated by these correlational diagrams.

As stated above, the hypotheses addressed are as follows:

H: The bacterial communities on lobsters with ESD are significantly different in quality and quantity than unaffected lobsters.

HA: The bacterial communities on the carapaces of healthy and shell-diseased lobsters are similar.

http://dx.doi.org/10.5772/63498

There are no major shifts in the microbiome between the Healthy and Diseased states, so we accept the alternative hypothesis and reject the original simple hypothesis. However, there are minor differences in the microbiomes of Healthy and Diseased lobsters. Furthermore, the microbiomes of lesion-free carapace on Diseased lobsters exhibited different microbiome compositions. However, the microbiomes of all three classes of the Diseased state that were identified here were similar enough that they occupied the same branches on a weighted UniFrac tree, and the difference between the microbiomes was determined to be statistically insignificant. Although there appears from these data to be a subtle difference between the microbiomes of samples from these three sample classes, the difference is not enough to fully support the original simple hypothesis. We must move forward with a more complicated hypothesis where environmental factors play a major role in the etiology of the disease. As such, we can start to define ESD as a complex environmental disease.

Arguably one of the most important advances in health and disease prevention has been the recognition that multiple pathogens are the cause of many diseases and it is now well accepted that these "polymicrobial disease" are in fact quite common [52]. As the body of knowledge has increased and we have extended our limits of detection and sequencing throughput, a growing number of diseases and syndromes have emerged that have been shown to be polymicrobial in nature. ESD is an example of one such polymicrobial disease.

This research has employed culture-independent techniques coupled with multivariate statistical treatment of the resultant data that present a shift in the lobster microbiome that correlates with the disease. This phenomenon is defined here as a dysbiosis. Although this research has elucidated this subtle shift in the microbiome of the lobster, it has not addressed the etiology of the disease. Indeed, it is not clear that the bacterial manifestations of this disease are anything more than a proximal cause. Researchers have successfully induced a condition that resembles ESD in captive lobsters but under extraordinary conditions. The evidence of involvement of alkylphenol contamination, for example, is circumstantial at this point. A direct evidence might be obtained through controlled experimentation as long as the confounding effects of captivity can eliminated.

The bulk method of extracting bacterial DNA from the lobster samples is itself confounding to the process of understanding the disease. Removing the biofilm and extracting the microbiomic DNA in bulk fashion precludes the interrogation of the spatial aspect of the biofilm. If microbes are cooperatively harvesting material and energy from a site, understanding their positional relationship may be useful. In addition, the nature of bulk extraction is that a relatively large amount of microbiota is captured. Such an approach can obscure members of the microbial community whose importance to the ecological function is disproportional to their relative abundance. It may be that minority members of the community, when observed in their spatial context within the biofilm, play a pivotal role in metabolic function. In the research described here, these bacteria may have been discarded due to insufficient abundance. *In situ* techniques, such as the use of laser capture microdissection on prepared sections of ESD lesions, coupled with DNA extraction of captured microbes, might shed some light on the spatial arrangements of the biofilm. In addition, visualization of intact biofilm colonies using confocal microscopy [24] combined with *in situ* hybridization techniques could

round out the picture in a way that would be the best of systems biology. In addition, the emergent field of metabolomics, the study of the net metabolic effects of epibiotic communities, would shed light on the changes in metabolic activity of a dysbiotic shift [48]. It is possible that what is described here is not a change in microbial organisms but merely a change in metabolic output of the same actors.

As noted previously, this research did not subdivide the disease lesions based on severity. Doing so would have yielded a more complete picture of the disease process and may have provided us with more insight into the roles of *Aquimarina* and *Jannaschia* and other taxa in the colonization of the lesions. A larger sample size, with more geographic diversity, would also be advantageous to increasing statistical confidence.

In response to the ESD crisis, a group of scientists, fisheries managers, and lobstermen formed the New England Lobster Health Initiative. It was this ad hoc committee that ultimately received funding that was awarded to several university and institutional researchers, including the award that funded what is reported here. The findings of each group were published as a special edition of the *Journal of Shellfish Research* [22]. Included in that edition was an article that summarizes some of what is contained herein [23]. A synthesis of all the research is summarized in the final article of the journal [53]. This research contributed a broad molecular-based survey that helped integrate studies such as those that elucidated immune response [20], potentially pathogenic microorganisms [12], gene expression [21], and xenobiotics [16]. Although the integration of these data is far from complete, there is sufficient evidence to suggest that ESD may represent a dysbiotic shift whose etiology could be alkylphenol intoxication.

Author details

Norman J. Meres

Address all correspondence to: normanmeres@mac.com

Yangzhou High School of Jiangsu Province, Yangzhou, China

References

[1] Pearce, J., and N. Balcom. The 1999 Long Island Sound lobster mortality event: Findings of a comprehensive research initiative. Journal of Shellfish Research. 2005, 24: 691–698.

[2] Zulkosky, A. M., J. P. Ruggieri, S. A. Terracciano, B. J. Brownawell, and A. E. McElroy. Acute toxicity of resmethrin, malathion and methoprene to larval and juvenile American lobsters (*Homarus americanus*) and analysis of pesticide levels in surface

waters after Scourge, Anvil and Altosid application. Journal of Shellfish Research. 2005, 24(3): 495–804.

[3] Smolowitz, R., A. Y. Chistoserdov, and A. Hsu. A description of the pathology of epizootic shell disease in the American lobster, *Homarus americanus*, H. Milne Edwards 1837. Journal of Shellfish Research. 2005, 24(3): 749–756.

[4] Hess, E. A shell disease in lobsters (*Homarus americanus*) caused by chitinovorous bacteria. Journal of the Biological Board of Canada. 1937, 3: 358–362.

[5] Sindermann, C. The Shell Disease Syndrome in Marine Crustaceans. NOAA Technical Memorandum. U.S. Department of Commerce, National Oceanic and Atmospheric Administration, National Marine Fisheries Service, Northeast Fisheries Center, Woods Hole, MA, 1989: 1–51.

[6] Kapareiko, D., J. Ziskowski, R. Robohm, A. Calabrese, and J. Pereira. Chitinoclasia prevalence on American lobster (*Homarus americanus*) populations in off-shore canyons located near the Deep-Water-Dumpsite 106 (DWD-106). Journal of Shellfish Research. 1997, 16(1): 319–320.

[7] Young, J. S., and J. B. Pearce. Shell disease in crabs and lobsters from New York bight. Marine Pollution Bulletin. 1975, 22: 101–105.

[8] Malloy, S. Bacteria induced shell disease of lobsters (*Homarus americanus*). Journal of Wildlife Diseases. 1978, 14: 2–10.

[9] Waddy, S. L., D. E. Aiken, and D. P. V. De Kleijn. Control of growth and reproduction. In: Factor, J. R. Biology of the Lobster, *Homarus americanus*. Academic Press, San Diego, CA, 1995: 217–266.

[10] Kunkel, J. R., W. Nagel, and M. J. Jercinovic. Mineral fine structure of the American lobster cuticle. Journal of Shellfish Research. 2012, 31(2): 515–526.

[11] Chistoserdov, A. Y., R. Smolowitz, F. Mirasol, and A. Hsu. Culture-dependent characterization of the microbial community associated with epizootic shell disease lesions in American lobster, *Homarus americanus*. Journal of Shellfish Research. 2005, 24(3): 741–747.

[12] Quinn, R., A. Metzler, R. Smolowitz, M. Tlusty, and A. Chisosterdov. Exposures of *Homarus americanus* shell to three bacteria isolated from naturally occurring epizootic shell disease lesions. Journal of Shellfish Research. 2012, 31(2): 485–493.

[13] Quinn, R., A. Metzler, M. Tlusty, R. Smolowitz, P. Leberg, and A. Chisosterdov. Lesion bacterial communities in American lobsters with diet-induced shell disease. Diseases of Aquatic Organisms. 2012, 98(3): 221–233.

[14] Bell, S. L., B. Allam, A. McElroy, A. Dove, and G. T. Taylor. Investigation of epizootic shell disease in American lobsters (*Homarus americanus*) from Long Island Sound I.

Characterization of associated microbial communities. Journal of Shellfish Research. 2012, 31(2): 473–484.

[15] Shields, J., K. Wheeler, and J. Moss. Histological assessment of the lobsters (*Homarus americanus*) in the "100 Lobsters" Project. Journal of Shellfish Research. 2012, 31(2): 439–447.

[16] Laufer, H., N. Demir, and X. Pan. Shell disease in the American lobster and its possible relation to alkyphenols. State of Lobster Science: Lobster Shell Disease Workshop. University of Massachusetts, Boston, MA, 2005.

[17] Biggers, W. J., and H. Laufer. Identification of juvenile hormone-active alkylphenols in the lobster *Homarus americanus* and in marine sediments. Biological Bulletin. 2004, 206: 13–24.

[18] Chang, E. S. Comparative endocrinology of molting and reproduction: Insects and crustaceans. Annual Review of Entomology. 1993, 38: 161–180.

[19] Laufer, H., M. Chen, M. Johnson, N. Demir, and J. M. Bobbitt. The effect of alkyphenols during lobster shell hardening. Journal of Shellfish Diseases. 2012, 31(2): 555–562.

[20] Homerding, M., A. McElroy, G. Taylor, A. Dove, and B. Allam. Investigation of epizootic shell disease in American lobsters (*Homarus americanus*) from Long Island Sound: II. Immune parameters in lobsters and relationships to the disease. Journal of Shellfish Research. 2012, 31(2): 495–504.

[21] Tarrant, A., D. Franks, and T. Verslycke. Gene expression in American lobster (*Homarus americanus*) with epizootic shell disease. Journal of Shellfish Research. 2012, 31(2): 505–513.

[22] Castro, K., J. Cobb, M. Gomez-Chiarri, and M. Tlusty. Preface. Journal of Shellfish Research. 2012, 31(2): 421–422.

[23] Meres, N., C. Ajuzie, M. Sikaroodi, M. Vemulapalli, J. Shields, and P. Gillevet. Dysbiosis in epizootic shell disease of the American lobster (*Homarus americanus*). Journal of Shellfish Research. 2012, 31(2): 463–472.

[24] Costerton, J. W. The Biofilm Primer. Springer, New York, 2007.

[25] Komanduri, S., P. M. Gillevet, M. Sikaroodi, E. Mutlu, and A. Keshavarzian. Dysbiosis in pouchitis; evidence of unique microfloral patterns in pouch inflammation. Clinical Gastroenterology and Hepatology. 2007, 5(3): 352–360.

[26] Lane, D. J. 16S/23S rRNA sequencing. In: Goodfellow, M. Nucleic Acid Techniques in Bacterial Systematics. John Wiley & Sons Ltd., West Sussex, England, 1991: 115–175.

[27] Gillevet, P. M. Multitag Sequencing and Ecogenomic Analysis, EPO 07871488.8; PCT/US2007/084840, BioSpherex LLC, 2006. Patent Number 8,603,749.

[28] Shields, J., K. Wheeler, J. Moss, B. Somers, and K. Castro. The "100 Lobsters" Project: A cooperative demonstration project for health assessments of lobsters from Rhode Island. Journal of Shellfish Research. 2012, 31(2): 431–438.

[29] Cole, J. R., Q. Wang, E. Cardenas, J. Fish, B. Chai, R. J. Farris, A. S. Kulam-Syed-Mohideen, D. M. McGarrell, T. Marsh, G. M. Garrity, and J. M. Tiedje. The Ribosomal Database Project: Improved alignments and new tools for rRNA analysis. Nucleic Acids Research. 2009, 37: 141–145.

[30] Caporaso, J., J. Kuczynski, J. Stombaugh, K. Bittinger, F. Bushman, E. Costello, N. Fierer, A. Pena, J. Goodrich, J. Gordon, G. Huttley, S. Kelley, D. Knights, J. Koenig, R. Ley, C. Lozupone, D. McDonald, B. Muegge, M. Pirrung, J. Reeder, J. Sevinsky, P. Turnbaugh, W. Walters, J. Widmann, T. Yatsunenko, J. Zaneveld, and R. Knight. QIIME allows analysis of high throughput community sequencing data. Nature Methods. 2010, 7(5): 335–336.

[31] Lanyon, S. Jackknifing and bootstrapping: Important "new" statistical techniques for ornithologists. The Auk. 1987, 104(1): 144–146.

[32] Lozupone, C., and R. Knight. UniFrac: A new phylogenetic method for comparing microbial communities. Applied and Environmental Microbiology. 2005, 71: 8228–8235.

[33] Davis, J. C. Statistics and Data Analysis in Geology. John Wiley & Sons, New York, NY, 2002.

[34] Garson, G. D. Discriminant Function Analysis. 2008. Available at: http://faculty.chass.ncsu.edu/garson/PA765/discrim.htm. Retrieved May 5, 2010.

[35] Klecka, W. R. Discriminant Analysis: Quantitative Applications in the Social Sciences. Sage Publications, Thousand Oaks, CA, 1980.

[36] Davey, M. E., and G. A. O'Toole. Microbial biofilms: From ecology to molecular genetics. Microbiology and Molecular Biology Reviews. 2000, 64(4): 847–867.

[37] Tsvetovat, M., and A. Kouznetsov. Social Network Analysis for Startups. O'Reilly Media, Sebastopol, CA, 2001.

[38] Smith, S. Investigating the intestinal microbiome and its host relationships in Ossabow pigs. Doctor of Philosophy dissertation, George Mason University, 2011.

[39] Shannon, P. A. M., O. Ozier, N. S. Balinga, J. T. Wang, D. Ramage, N. Amin, B. Schwikoski, and T. Ideker. Cytoscape: A software environment for integrated models of biomolecular interaction networks. Genome Research. 2003, 13(11): 2498–2504.

[40] Shannon, C. A mathematical theory of communication. The Bell System Technical Journal. 1948, 27: 379–423.

[41] Watts, D., and S. Strogatz. Collective dynamics of "small world" networks. Nature. 4 June 1998: 440–442

[42] Wagner-Döbler, I., H. Rheims, A. Felske, R. Pukall, and B. Tindall. *Jannaschia helgolandensis* gen. nov., sp. nov., a novel abundant member of the marine *Roseobacter* clade from the North Sea. International Journal of Systematic and Evolutionary Microbiology. 2003, 53: 731–738.

[43] Nedashkovskaya, O., M. Vancanneyt, L. Christiaens, N. Kalinovskaya, V. Mikhailov, and J. Swings. *Aquimarina intermedia* sp. nov., reclassification of *Stanierella latercula* (Lewin 1969) as *Aquimarina latercula* comb. nov. and *Gaetbulimicrobium brevivitae* Yoon et al. 2006 as *Aquiimarina brevivitae* comb. nov. and emended description of the genus *Aquimarina*. International Journal of Systematic and Evolutionary Microbiology. 2006, 56: 2037–2041.

[44] Malani, A., D. Aronoff, S. Bradley, and C. Kauffman. *Cardiobacterium hominis* endocarditis: Two cases and a review of the literature. European Journal of Clinical Microbiology & Infectious Diseases. 2006, 25(9): 587–595.

[45] Arahal, D., M. Macían, E. Garay, and M. Pujalte. *Thalassobius mediterraneus* gen. nov., sp. nov., and reclassification of *Ruegeria gelatinovorans* as *Thalassobius gelatinovorus* comb. nov. International Journal of Systematic and Evolutionary Microbiology. 2005, 55: 2371–2376.

[46] Van Trappen, S., J. Mergaert, and J. Swings. *Loktanella salsilacus* gen. nov., sp. nov., *Loktanella fryxellensis* sp. nov., and *Loktanella vestfoldensis* sp. nov., new members of the *Rhodobacter* group isotaled from microbial mats in Antarctic lakes. International Journal of Systematic and Evolutionary Microbiology. 2004, 54: 1263–1269.

[47] Schumann, P., P. Kämpfer, H.-J. Busse, and L. Evtushenko. Proposed minimal standards for describing new genera and species of the suborder *Micrococcineae*. International Journal of Systematic and Evolutionary Microbiology. 2009, 59: 1823–1849.

[48] Wahl, M., F. Goecke, A. Labes, S. Dobretsov, and F. Weinberger. The second skin: Ecological role of epibiotic biofilms on marine organisms. Frontiers in Microbiology. 2012, 3(292): 1–21.

[49] Orr, J., V. Fabry, O. Aumont, L. Bopp, S. Doney, R. Feely, A. Gnanadesikan, N. Gruber, A. Ishida, F. Joos, R. Key, K. Lindsay, E. Maier-Reimer, R. Matear, P. Monfray, A. Mouchet, R. Najjar, G. Plattner, K. Rodgers, C. Sabine, J. Sarmiento, R. Schlitzer, R. Slater, I. Totterdell, M. Weirig, Y. Yamanaka, and A. Yool. Anthropogenic ocean acidification over the twenty-first century and its impact on calcifying organisms. Nature. 2005, 437: 681–686.

[50] Bourne, D., L. Høj, N. Webster, J. Swan, and M. Hall. Biofilm development within a larval rearing tank of the tropical rock lobster, *Panulirus ornatus*. Aquaculture. 2006, 260: 27–38.

[51] Welsh, J., P. King, and E. MacCarthy. Characterization of a biofilm bacterium from a recirculation system for European lobster (*Homarus gammarus*). Aquaculture. 2011, 318: 458–463.

[52] Brogden, K., and J. Guthmiller. Polymicrobial Diseases. ASM Press, Washington, DC, 2002.

[53] Gomez-Chiarri, M., and S. Cobb. Shell disease in the American lobster, *Homarus americanus*: A synthesis of research from the New England Lobster Research Initiative: Lobster shell disease. Journal of Shellfish Research. 2012, 31(2): 583–590.

IntechOpen